UNIVERSIDADE DE SÃO PAULO
FACULDADE DE ODONTOLOGIA DE BAURU

ALINE DIONIZIO VALLE

Proteomic analysis of jejunum and ileum in rats exposed to acute or chronic fluoride dose

BAURU
2020

ALINE DIONIZIO VALLE

Proteomic analysis of jejunum and ileum in rats exposed to acute or chronic fluoride dose

Análise proteômica do jejuno e íleo em ratos expostos a dose aguda ou crônica de fluoreto

Thesis presented to the Bauru School of Dentistry of the University of São Paulo to obtain the degree of PhD in Science in the Applied Dental Science Program, Oral Biology, Stomatology, Radiology and Imaging concentration area.

Supervisor: Prof. Dr. Marília Afonso Rabelo Buzalaf

Tese apresentada à Faculdade de Odontologia de Bauru da Universidade de São Paulo para obtenção do título de Doutor em Ciências no Programa de Ciências Odontológicas Aplicadas, área de concentração Biologia Oral, Estomatologia, Radiologia e Imaginologia.

Orientadora: Profa. Dra. Marília Afonso Rabelo Buzalaf

Versão Corrigida

BAURU
2020

Valle, Aline Dionizio
Proteomic analysis of jejunum and ileum in rats exposed to acute or chronic fluoride dose/ Aline Dionizio Valle. – Bauru, 2020.
164p. : il. ; 31cm.

Tese (Doutorado) – Faculdade de Odontologia de Bauru. Universidade de São Paulo

Orientadora: Prof. Dr[a] Marilia Afonso Rabelo Buzalaf

Nota: A versão original desta tese encontra-se disponível no Serviço de Biblioteca e Documentação da Faculdade de Odontologia de Bauru – FOB/USP.

Comitê de Ética em Animais da FOB-USP

Protocolo nº: 014/2011 e 012/2016

Data: 28/06/2011 e 25/05/2016

(Cole a cópia de sua folha de aprovação aqui)

DEDICATÓRIA

Dedico esta tese à minha família e meu marido,

Aos meus pais **Rubens** e **Lucimar**,

Minha base, meus maiores exemplos, sempre me apoiaram, me incentivaram a lutar pelos meus objetivos, sempre com muita dedicação e amor incondicional, a mim dedicado.

À minha irmã **Amanda**,

Agradeço por mesmo de longe sempre estar presente me ajudando, incentivando e me apoiando.

Ao meu marido **Cesar**,

Meu amor, meu amigo, pessoa que me acalma e me incentiva. Obrigada por sempre estar ao meu lado, me fazendo rir e me fazendo ser forte. Hoje meu incentivo é a nossa família!

AGRADECIMENTOS

Agradeço primeiramente a **Deus e Maria**.

Eles que me concedeu o dom da vida, que esrão presentes em todos os momentos me dando força e luz para trilhar meus objetivos. Levanto todas as manhãs agradecendo por mais um dia, pois me ensinam que tropeçar é um aprendizado e que são nos tropeços da vida que mais aprendemos.

Aos meus pais **Rubens** e **Lucimar.**

Obrigada por sermos uma família, a qual sei que posso contar a qualquer hora, para qualquer situação, por mais difícil que seja, estão ao meu lado, ou puxando a orelha ou me abraçando e me dando palavras de carinho. Obrigada por me ensinarem a nunca desistir e me dizer que não seria fácil, mas que seria possível, se me dedicasse. Neste trabalho, vocês fizeram parte a todo momento, me levando a faculdade, me incentivando, cuidando da minha saúde, me fazendo rir quando estava preocupada, enfim, obrigada por serem quem são, e serem os meus pais, amo vocês infinitamente. São meus maiores orgulhos

À minha irmã **Amanda.**

Imagino o quão difícil é você estar tão longe de nós e te admiro por isso, obrigada por mesmo de longe sempre me ajudar, obrigada por me apoiar, ser amiga e irmã. Te amo!

Ao meu marido **Cesar.**

Obrigada por ser meu acalanto e meu porto seguro em momentos de nervoso, de desespeiro com as análises, prazos, etc, afinal eu sou ligada no 220v e por muitas vezes preciso desacelerar. Não tenho palavras pra descrever o quão importante você é para mim, durante esses quatro anos, em meio a loucura de um doutorado nos casamos e nos tornamos uma família, a qual é por ela que me dedico e busco cada dia melhorar mais e mais. Obrigada por tudo e principalmente por me ensinar que o amor e companheirismo está acima de qualquer coisa. Te amo vida!

Ao meu **cunhado Samuel**

Obrigada por fazer parte da nossa família, e principalmente por cuidar tão bem da minha irmã. Além claro, de sempre compartilhar dos momentos do meu doutorado, se preocupando e aconselhando.

À minha **avó Zenaide**

Vó, madrinha, muito obrigada por sempre cuidar de mim e vibrar a cada conquista, me ensinar que nada é fácil, mas que um dia sempre colhemos a recompensa. A senhora é um exemplo de força e dedicação pela família, se Deus permitir seguirei seus passos!

Ao Tio **Ricardo**

O primeiro cientista da família, quem sempre me apoiou e vibrou comigo a cada passo dado no âmbito acadêmico. Obrigada por vibrar comigo cada conquista e sempre que necessário me ajudar para chegar até aqui.

Aos **"tops"** e **"jogatina"** família e amigos.

Neste percurso estiveram ao meu lado, brincando comigo, me fazendo rir para desestressar e minimizar. Obrigada pelo carinho e amizade. E por serem minha família. Aqueles que escolhi para viver lado a lado.

A família **Souza Valle.**

Sogra, sogro, cunhados e cunhadas. Obrigada por fazerem parte dos meus dias neste período, por serem minha segunda família.

À minha amiga **Isabela e Beatriz**

Esse ano além de uma tese, comemoro com vocês uma década de amizade. Quem diria, aquelas companheiras de bancada no laboratório se tornariam mais que amigas, se tornaria comadres. Agradeço por sempre me ajudarem e estarem presentes nos meus dias, seja pra eu desabafar, me ajudarem nos tropeços de uma tese, me fazerem dar risada, tomar café, passear, enfim. Nossa amizade cresceu e se fortificou, amigo é presente de Deus e devemos cuidar, com certeza cuidarei para que nunca se acabe.

À **minha amiga Heloisa**.

Helo, com você aprendi muito, da iniciação ao mestrado como minha co-orientadora. E hoje como minha amiga, além de todo aprendizado profissional, aprendi com você a compartilhar meu conhecimento, a ser humilde e pedir ajuda, e principalmente não desistir. Te admiro muito e te quero sempre perto.

À minhas amigas **Tamara, Tati e Ju Trevizol.**

Meninas, muito obrigada por sempre estarem presente e serem tão prestativas, sempre se propondo a me ajudar e aprenderem. Considero vocês muito mais que amigas de laboratório, considero amigas da vida, quero ter vocês sempre por perto.

Aos meus colegas do **laboratório de bioquímica.**

Técnicas Larissa e Thelma, e alunos amigos, obrigada por cada um me ensinar um pouquinho do tanto que sabe, e por dividirem risadas, isso contribuiu e contribuirá muito para minha formação. Obrigada pelo carinho e companhia em todos esses dias.

Aos professores **Rodrigo e Ana Carolina.**

Agradeço por todo ensinamento, nestes 10 anos aprendi muito com vocês. Saibam que farei o possível para colocar em prática cada detalhe ensinado por vocês.

Ao professor **Rafael Lima**, **Leo e amigas da UFPA**

Não tenho palavras pra expressar minha admiração e minha gratidão. Fazer parte do grupo de vocês me fez aprender e crescer muito profissionalmente. Vocês são demais! Parabéns por quão bem conduz seus estudos e alunos Rafa!

Aos **funcionários do Biotério**

Obrigada por me ajudarem com os cuidados dos animais, me auxiliando e me instruindo da melhor forma.

À **Faculdade de Odontologia de Bauru-USP**, na pessoa do senhor diretor **Prof. Dr. Carlos Ferreira do Santos** e da senhora presidente da **Comissão de Pós-Graduação, Profa. Dra. Izabel Regina Fischer Rubira de Bullen,** pela oportunidade em realizar pós-graduação em nível de Doutorado nesta instituição, ao qual tenho orgulho e profundo respeito. Muito obrigada.

À **Fundação de Amparo à Pesquisa do Estado de São Paulo (FAPESP)**, pelo apoio financeiro concedido durante a realização deste estudo de Doutorado.

Ao **CNPq,** pelo apoio financeiro inicial deste projeto, que foi fundamental para o desenvolvimento desse trabalho.

AGRADECIMENTOS ESPECIAIS

À professora Marília Afonso Rabelo Buzalaf da Faculdade de Odontologia de Bauru. Esse ano completo 10 anos no laboratório de bioquímica, durante essa década foram um ano de estágio, três iniciações científicas, um estágio no exterior, dois anos de mestrado e 4 anos de doutorado, e todos orientados pela senhora. Durante esse período, incluindo o primeiro contato que tivemos, sempre se mostrou ser uma pessoa maravilhosa, que não mede esforços para compartilhar suas conquistas e conhecimentos com os alunos, que torce e vibra por nós a cada vitória e trabalho apresentado. Nestes anos também pude ver que além de nossa orientadora também é mãe, esposa, filha, empresária, professora e pesquisadora, e que mesmo com tantos afazeres, não deixa se de dedicar a eles e a nós (alunos).

Segundo o dicionário professor é “Pessoa que, por conhecimento adquirido ou experiência de vida, pode ser mentor, espelho e ou norte para outros que desconhecem fatos ou acontecimentos”. Com toda certeza a senhora faz jus a este significado. Outra frase que elucida muito bem a senhora é “Eu nunca poderia pensar em educação sem amor. É por isso que me considero um educador: acima de tudo porque sinto amor.” *Paulo Freire*. A senhora transmite no olhar o amor pelos alunos e pelo que faz, com certeza assim, tudo fica mais tranquilo e mais satisfatório. Além disso nos encoraja, nos mostra que mesmo com tantos compromissos sempre é possível encontrarmos um horário para fazermos e aprendermos coisas novas, a senhora é nosso exemplo de profissional e de pessoa.

Obrigada imensamente, por toda oportunidade que me destes, por toda confiança que depositastes em mim e ainda depositas. Através da senhora pude conhecer o lado acadêmico e da pesquisa mais de perto, participar ativamente das atividades, e descobrir a minha admiração pela pesquisa. A senhora com certeza foi peça fundamental para que eu me tornasse hoje a profissional que sou.

Que Deus e Nossa Senhora, continuem lhe abençoando e guiando, para que continue essa profissional e pessoa que é conquistando cada dia mais seus objetivos e realizações.

“As nuvens mudam sempre de posição, mas são sempre nuvens no céu.
Assim devemos ser todo dia, mutantes,
porém leais com o que pensamos
e sonhamos” (Paulo Beleki).

ABSTRACT

Proteomic analysis of jejunum and ileum in rats exposed to acute or chronic fluoride dose.

The gastrointestinal tract (GIT) is considered the main route of exposure to fluoride (F), which is rapidly absorbed from it. Exposure to this ion can generate considerable changes in the morphology of the intestine, which can affect its functions, leading to gastrointestinal symptoms that represent the first signs of F toxicity. In previous studies performed by our research group, it was observed that exposure to F interferes significantly in the expression of several proteins in the duodenum. Due to the distinct anatomical, histological and physiological characteristics found among the different distinct segments of the small intestine, the present study aimed to evaluate the effect of acute or chronic exposure to F on the proteomic profile of the jejunum and the ileum of rats. Male 60-day-old *Wistar* rats were treated for 30 days with chronic doses of 0 mgF/L, 10 mgF/L or 50 mgF/L. The acute dose of F (25 mg/Kg body weight) or deionized water (control) was administered once by gastric gavage. After the experimental periods, the jejunum and the ileum were collected. Proteomic analysis of both segments was performed using the nanoACQUITY UPLC-Xevo QTof MS system (Waters, Manchester, UK), in order to better understand the mechanisms involved in acute or chronic F toxicity, which led to the morphological changes observed in our previous studies. The difference in expression between the groups was obtained using the PLGS software, considering $p<0.05$ and $1\text{-}p>0.95$ for the for the down and upregulated proteins, respectively. Under acute exposure to F, most of the proteins with altered expression were upregulated in the group 25 mg/Kg F *vs.* Control. Our results, when analyzed together (jejunum and ileum), suggest that the gastrointestinal symptoms found in these cases may be related to inhibition of protein synthesis by exposure to a high dose of F, such as changes in proteins that regulate the cytoskeleton and energy metabolism, mainly in carbohydrate metabolism. Under chronic exposure to F, most of the proteins with altered expression were upregulated in the group 10 mgF/L *vs.* control and in the comparison 50 mgF/L *vs.* control. In the jejunum, there were changes in the abundance of several proteins correlated with

protein synthesis, glucose homeostasis, energy metabolism and neural functions. Moreover, in the ileum, a decrease in gastrotropin was found, which may be associated with diarrhea, a common symptom found in cases of F toxicity. In addition, changes in different myosin isoforms were observed, which might have contributed to the structural alterations found in the histological analysis previously performed. In conclusion, acute exposure to F mostly downregulates several proteins, with emphasis on partners involved in protein synthesis, cytoskeleton and energy metabolism, which might help explain the gastrointestinal symptons found in cases of acute exposure to this ion. Distinctly from which was observed for the acute treatment, under chronic treatment with both F concentrations an increase in the expression of proteins was observed, which might indicate an adaptation of the body, in attempt to fight the deleterious effects of this ion.

Key-words: Fluoride. Ileum. Jejunum. Proteomic analysis. Chronic exposure. Acute exposure.

RESUMO

Análise proteômica do jejuno e íleo em ratos expostos a dose aguda ou crônica de fluoreto.

O trato gastrointestinal (TGI) é considerado a principal via de exposição ao fluoreto (F), que é rapidamente absorvido por ele. A exposição a esse íon pode gerar alterações consideráveis na morfologia do intestino, o que pode afetar suas funções, levando a sintomas gastrointestinais que representam os primeiros sinais de toxicidade do F. Em estudos anteriores realizados pelo nosso grupo de pesquisa, observou-se que a exposição ao F interfere significativamente na expressão de várias proteínas no duodeno. Devido às distintas características anatômicas, histológicas e fisiológicas encontradas entre os diferentes segmentos do intestino delgado, o presente estudo teve como objetivo avaliar o efeito da exposição aguda ou crônica a F no perfil proteômico do jejuno e íleo de ratos. Ratos Wistar machos de 60 dias de idade foram tratados por 30 dias com doses crônicas de 0 mgF/L, 10 mgF/L ou 50 mgF/L. A dose aguda de F (25 mg/kg de peso corporal) ou água deionizada (controle), foram administradas uma única vez, por gavagem gástrica. Após os períodos experimentais, o jejuno e o íleo foram coletados. A análise proteômica de ambos os segmentos foi realizada com o sistema nanoACQUITY UPLC-Xevo QTof MS (Waters, Manchester, Reino Unido), a fim de melhor compreender os mecanismos envolvidos na toxicidade aguda ou crônica da F, o que levou às alterações morfológicas observadas em nossos estudos anteriores. A diferença de expressão entre os grupos foi obtida no software PLGS, considerando $p < 0.05$ e $1\text{-}p > 0.95$ para as proteínas sub e supraregulada, respectivamente. Sob exposição aguda a F, a maioria das proteínas com expressão alterada foi aumentada no grupo 25 mg/Kg F *vs.* Controle. Nossos resultados, quando analisados em conjunto (jejuno e íleo), sugerem que os sintomas gastrointestinais encontrados nesses casos podem estar relacionados à inibição da síntese de proteínas pela exposição a uma alta dose de F, como alterações nas proteínas que regulam o citoesqueleto e o metabolismo energético, principalmente no metabolismo de carboidratos. Sob exposição crônica a F, a maioria das proteínas com expressão alterada foi aumentada no grupo 10 mgF/L *vs.* controle e na comparação 50 mgF/L *vs.* controle. No jejuno, houve alterações na abundância de várias proteínas correlacionadas com a síntese de proteínas, homeostase da glicose, metabolismo

energético e funções neurais. Além disso, no íleo, foi encontrada uma diminuição da gastrotropina, que pode estar associada à diarreia, sintoma comum encontrado nos casos de toxicidade por F. Em adição, foram observadas alterações nas diferentes isoformas da miosina, o que pode ter contribuído para as alterações estruturais encontradas na análise histológica realizada anteriormente. Em conclusão, a exposição aguda ao F na maioria das vezes regula negativamente várias proteínas, com ênfase nos parceiros envolvidos na síntese de proteínas, no citoesqueleto e no metabolismo energético, o que pode ajudar a explicar os sintomas gastrointestinais encontrados nos casos de exposição aguda a esse íon. Distintamente do que foi observado no tratamento agudo, no tratamento crônico com ambas as concentrações de F foi observado um aumento na expressão de proteínas, o que pode indicar uma adaptação do corpo, na tentativa de combater os efeitos deletérios desse íon.

Palavras-chave: Fluoreto. Íleo. Jejuno. Análise proteômica. Exposição crônica. Exposição aguda.

SUMÁRIO

1 INTRODUCTION

1 INTRODUCTION

Fluorine is the thirteenth most abundant element in the earth's crust (SHANTHAKUMARI; SRINIVASALU; SUBRAMANIAN, 2004). It the form of is negatively charged ion, called fluoride (F), it is important for many physiological cellular processes in the organism (YAN *et al.*, 2011). F is present in biological fluids and tissues as a trace element and 99% of the F in the organism is accumulated in the hard tissues. F can also be artificially added to the drinking water and fluoridated dental products, which together are the main source of F for human consumption (BUZALAF, 2018; BUZALAF; WHITFORD, 2011).

Because of its widely known ability to control dental caries, since the 1940´s many cities worldwide have adopted artificial fluoridation of drinking water as a standard public health policy (IHEOZOR-EJIOFOR *et al.*, 2015). In Brazil, since 1974, artificial fluoridation of water from public supply is mandatory in cities where there is water treatment station and this is regulated by law (Brazil, Ministry of Health, Decree nº76872, 1975; Brazil, Ministry of Health, Federal Law Nº. 6050.1974)(BRASIL, 1974; 1976). However, since F is an element naturally found in water, in some cities the concentration naturally found is above the recommended limits (0.7 – 1.2 mgF/L), which can cause deleterious effects (WHITFORD, 1996). Among these effects, the most known is fluorosis, which can be dental (DENBESTEN; LI, 2011) or skeletal (KRISHNAMACHARI, 1986). A plethora of experimental studies attest that, when F is administered to animals in high doses, distinct alterations in different tissues affecting diverse proteins and enzymes are found (ARAUJO *et al.*, 2019; BARBIER; ARREOLA-MENDOZA; DEL RAZO, 2010; CARVALHO *et al.*, 2013; KOBAYASHI *et al.*, 2014; KOBAYASHI *et al.*, 2009; LIMA LEITE *et al.*, 2014; LOBO *et al.*, 2015; PEREIRA *et al.*, 2018; PEREIRA *et al.*, 2016; PEREIRA *et al.*, 2013; STRUNECKA *et al.*, 2007). Among these tissues, morphological and proteomic changes were found in the jejunum (DIONIZIO *et al.*, 2018) and duodenum (MELO *et al.*, 2017) of rats. This is expected, since most of the F is absorbed from the small intestine (NOPAKUN; MESSER, 1990; NOPAKUN; MESSER; VOLLER, 1989) .

Several researches with different designs (in vitro laboratory studies and in vivo animal and human studies) have shown that F has a toxic effect, which is related to the amount and timing of exposure (BARBIER; ARREOLA-MENDOZA; DEL RAZO,

2010; PEREIRA *et al.*, 2018). This effect can be classified as acute or chronic (for review see (DENBESTEN; LI, 2011; WHITFORD, 1992; 2011).

Acute toxicity occurs by ingesting a large amount of F at a single time. The signs and symptoms related to this type of intoxication are vomiting with blood, diarrhea, bronchospasm, ventricular fibrillation, dilated pupils, hemoptysis, cramps, cardiac collapse, hypercalcemia, hypocalcemia and impaired renal function. In the literature, we found both accidental and intentional cases of acute F toxicity (WHITFORD, 1992; 2011).

Chronic toxicity occurs when above-the-optimal F concentrations are ingested over a certain period of time (DENBESTEN; LI, 2011). The main sources of chronic F intake are water and dentifrice. Despite daily ingestion of F in the range between 0.05 and 0.07 mg/kg body weight/ day is still recognized as the optimal level of F intake, the precise level of daily F intake able to control caries and that is not associated with increased risk of dental fluorosis is not known so far (BUZALAF, 2018).

After ingestion, F can cross the cell membranes mainly by diffusion of its weak acid (HF) (BUZALAF; WHITFORD, 2011), causing adverse effects by invading soft tissues such as brain, liver, intestine, heart and lung, with several structural and metabolic changes being observed after its excessive administration (BARBIER; ARREOLA-MENDOZA; DEL RAZO, 2010; CHOUHAN; FLORA, 2008) (INKIELEWICZ-STEPNIAK; CZARNOWSKI, 2010). In general, it is recognized that the toxic effects of F are due mainly to enzymatic inhibition, destruction of collagen, paralysis of activities of the immune system and damage to the gastrointestinal tract (GIT) (CHOUHAN; FLORA, 2008).

Being the main route of F absorption, the GIT can be exposed to high concentrations of F daily (BUZALAF; WHITFORD, 2011), which and can lead to considerable changes in the morphology of the intestine, which in turn affects its functions (CHAUHAN; OJHA; MAHMOOD, 2011; DIONIZIO *et al.*, 2018; MELO *et al.*, 2017). Moreover, the complex functions of the GIT, which include mixing and spreading food, providing digestive enzymes, reabsorption and secretion, as well as maintaining adequate blood flow levels, depend on intense coordination of autonomic neuronal networks (COOKE, 2000; FURNESS *et al.*, 1995). These networks are embedded in the walls of the intestine and are formed by the interconnection of ganglionic and aganglionic plexuses and also over a highly sophisticated network of

polysynaptic circuits (FURNESS *et al.*, 2004), this large set being called Enteric Nervous System (ENS) (SCHAFER; VAN GINNEKEN; COPRAY, 2009).

In a recent study, our research group evaluated the effect of acute or chronic exposure to F, on the general population of enteric neurons and on the subpopulations that express the main enteric neurotransmitters in the duodenum, jejunum and ileum. Relevant changes were found (MELO, 2015; MELO *et al.*, 2017). This study also reported important proteomic alterations in the duodenum of rats treated with F. Among them are: 1) F, when chronically administered in the dose of 10 mg/L through the drinking water, altered the expression of 229 proteins, among which most where upregulated when compared to the control group (deionized water), being the "pyridine metabolism" the most affected biological process (MELO *et al.*, 2017); 2) F altered the expression of 284 proteins after chronic exposure to water containing 50 mgF/L when compared with control, being "protein polymerization" the mostly affected biological process (MELO *et al.*, 2017); 3) After acute administration of F in the dose of 25 mg/kg (gastric gavage), F altered the expression of 356 proteins with the vast majority of these proteins having their expression downregulated and the mostly affected biological process was "generation of precursors and energy" (MELO, 2015). It is important to highlight that both under acute and chronic F exposure, the effect of F in the duodenum was much more pronounced than that observed in proteomic studies conducted with other organs, such as kidneys (DE CARVALHO *et al.*, 2013; KOBAYASHI *et al.*, 2009; XU *et al.*, 2005), brain (GE *et al.*, 2011; NIU *et al.*, 2014) and liver (ARAUJO *et al.*, 2019; DIONIZIO *et al.*, 2019; KHAN *et al.*, 2019; PEREIRA *et al.*, 2018; PEREIRA *et al.*, 2013), even with similar doses of F. The most probable reason for the higher susceptibility of the duodenum to the effects of F, when compared to the other organs, lies on the fact that 70-75% of the absorption of F occurs in the small intestine (NOPAKUN; MESSER, 1990; NOPAKUN; MESSER; VOLLER, 1989). Consequently, when a certain dose of F is ingested, the cells in the intestinal wall are exposed to a higher concentration of F than the cells of the other organs, which will come into contact only with the F that is absorbed (BUZALAF; WHITFORD, 2011).

Due to the distinct anatomical, histological and physiological characteristics found among the different distinct segments of the small intestine (GUYTON; HALL, 2015) and considering the important changes observed in the general population of neurons in the jejunum and ileum and in subpopulations that express the main enteric neurotransmitters in our previous study (MELO, 2015), it is extremely important to

perform proteomic analysis of these two intestinal segments, in order to obtain information about the possible mechanisms involved in the alteration of the ENS by exposure to F, which may explain the gastrointestinal symptoms caused by this exposure.

1.1 OBJECTIVES

The general aim of this study was to investigate the effect of acute or chronic exposure to F on the protein expression profile of the jejunum and ileum of rats, using proteomic analyses. Moreover, protemics findings were associated with the morphological alterations in the SNE performed in a previous study (Melo et al. 2015), in order to provide mechanistic rationale to explain the gastrointestinal symptoms caused by F.

REFERENCES

REFERENCES

ARAUJO, T. T.; BARBOSA SILVA PEREIRA, H. A.; DIONIZIO, A.; SANCHEZ, C. D. C. *et al.* Changes in energy metabolism induced by fluoride: Insights from inside the mitochondria. **Chemosphere**, 236, p. 124357, Jul 12 2019.

ARTMAN, L.; DORMOY-RACLET, V.; VON RORETZ, C.; GALLOUZI, I. E. Planning your every move: the role of beta-actin and its post-transcriptional regulation in cell motility. **Semin Cell Dev Biol**, 34, p. 33-43, Oct 2014.

BALESARIA, S.; PELL, R. J.; ABBOTT, L. J.; TASLEEM, A. *et al.* Exploring possible mechanisms for primary bile acid malabsorption: evidence for different regulation of ileal bile acid transporter transcripts in chronic diarrhoea. **Eur J Gastroenterol Hepatol**, 20, n. 5, p. 413-422, May 2008.

BARBIER, O.; ARREOLA-MENDOZA, L.; DEL RAZO, L. M. Molecular mechanisms of fluoride toxicity. **Chem Biol Interact**, 188, n. 2, p. 319-333, Nov 5 2010.

BASSIN, E. B.; WYPIJ, D.; DAVIS, R. B.; MITTLEMAN, M. A. Age-specific fluoride exposure in drinking water and osteosarcoma (United States). **Cancer Causes Control**, 17, n. 4, p. 421-428, May 2006.

BENARROCH, E. E. Enteric Nervous System - Functional organization and neurologic implications. **Neurology**, 69, n. 20, p. 1953-1957, Nov 13 2007.

BOGDANI, M.; HENSCHEL, A. M.; KANSRA, S.; FULLER, J. M. *et al.* Biobreeding rat islets exhibit reduced antioxidative defense and N-acetyl cysteine treatment delays type 1 diabetes. **J Endocrinol**, 216, n. 2, p. 111-123, Feb 2013.

BRASIL. Lei nº 6.050, de 24 de maio de 1974. Dispõe sobre a obrigatoriedade da fluoretação das águas em sistemas de abastecimento. SAÚDE, M. d. Brasilia - Distrito Federal: Diario oficial da República Federativa do Brasil. 8**:** 687-688 p. 1974.

BRASIL. Decreto n º 76.872, de 22 de dezembro de 1975. Regulamenta a Lei n º 6.050, de 24 de maio de 1974, que dispõe sobre a fluoretação da água em sistemas públicos de abastecimento. . SAÚDE, M. d. Brasilia - Distrito Federal: Coleção das Leis de 1975. 8**:** 687-688 p. 1976.

BREWER, P. D.; HABTEMICHAEL, E. N.; ROMENSKAIA, I.; COSTER, A. C. *et al.* Rab14 limits the sorting of Glut4 from endosomes into insulin-sensitive regulated

secretory compartments in adipocytes. **Biochem J**, 473, n. 10, p. 1315-1327, May 15 2016.

BUZALAF, M. A. R. Review of Fluoride Intake and Appropriateness of Current Guidelines. **Adv Dent Res**, 29, n. 2, p. 157-166, Mar 2018.

BUZALAF, M. A. R.; WHITFORD, G. M. Fluoride metabolism. **Monogr Oral Sci**, 22, p. 20-36, 2011.

CARVALHO, J. G.; LEITE ADE, L.; PERES-BUZALAF, C.; SALVATO, F. *et al.* Renal proteome in mice with different susceptibilities to fluorosis. **PLoS One**, 8, n. 1, p. e53261, 2013.

CHAUHAN, S. S.; OJHA, S.; MAHMOOD, A. Modulation of lipid peroxidation and antioxidant defense systems in rat intestine by subchronic fluoride and ethanol administration. **Alcohol**, 45, n. 7, p. 663-672, Nov 2011.

CHOUHAN, S.; FLORA, S. J. Effects of fluoride on the tissue oxidative stress and apoptosis in rats: biochemical assays supported by IR spectroscopy data. **Toxicology**, 254, n. 1-2, p. 61-67, Dec 5 2008.

CHU, J.; PHAM, N. T.; OLATE, N.; KISLITSYNA, K. *et al.* Biphasic regulation of myosin light chain phosphorylation by p21-activated kinase modulates intestinal smooth muscle contractility. **J Biol Chem**, 288, n. 2, p. 1200-1213, Jan 11 2013.

COOKE, H. J. Neurotransmitters in neuronal reflexes regulating intestinal secretion. **Ann N Y Acad Sci**, 915, p. 77-80, 2000.

DAVIS, R. A.; ATTIE, A. D. Deletion of the ileal basolateral bile acid transporter identifies the cellular sentinels that regulate the bile acid pool. **Proc Natl Acad Sci U S A**, 105, n. 13, p. 4965-4966, Apr 1 2008.

DE CARVALHO, C. A.; ZANLORENZI NICODEMO, C. A.; FERREIRA MERCADANTE, D. C.; DE CARVALHO, F. S. *et al.* Dental fluorosis in the primary dentition and intake of manufactured soy-based foods with fluoride. **Clin Nutr**, 32, n. 3, p. 432-437, Jun 2013.

DENBESTEN, P.; LI, W. Chronic fluoride toxicity: dental fluorosis. **Monogr Oral Sci**, 22, p. 81-96, 2011.

DEY, S.; SWARUP, D.; SAXENA, A.; DAN, A. In vivo efficacy of tamarind (Tamarindus indica) fruit extract on experimental fluoride exposure in rats. **Res Vet Sci**, 91, n. 3, p. 422-425, Dec 2011.

DIONIZIO, A.; PEREIRA, H.; ARAUJO, T. T.; SABINO-ARIAS, I. T. *et al.* Effect of Duration of Exposure to Fluoride and Type of Diet on Lipid Parameters and De Novo Lipogenesis. **Biol Trace Elem Res**, 190, n. 1, p. 157-171, Jul 2019.

DIONIZIO, A. S.; MELO, C. G. S.; SABINO-ARIAS, I. T.; VENTURA, T. M. S. *et al.* Chronic treatment with fluoride affects the jejunum: insights from proteomics and enteric innervation analysis. **Sci Rep**, 8, n. 1, p. 3180, Feb 16 2018.

DUNIPACE, A. J.; KELLY, S. A.; WILSON, M. E.; ZHANG, W. *et al.* Correlation of Fluoride Levels in Human Plasma, Urine and Saliva. **Journal of Dental Research**, 74, p. 134-134, 1995.

FOLLIN-ARBELET, B.; MOUM, B. Fluoride: a risk factor for inflammatory bowel disease? **Scand J Gastroenterol**, 51, n. 9, p. 1019-1024, Sep 2016.

FURNESS, J. B.; JOHNSON, P. J.; POMPOLO, S.; BORNSTEIN, J. C. Evidence that enteric motility reflexes can be initiated through entirely intrinsic mechanisms in the guinea-pig small intestine. **Neurogastroenterol Motil**, 7, n. 2, p. 89-96, Jun 1995.

FURNESS, J. B.; JONES, C.; NURGALI, K.; CLERC, N. Intrinsic primary afferent neurons and nerve circuits within the intestine. **Prog Neurobiol**, 72, n. 2, p. 143-164, Feb 2004.

GE, Y.; NIU, R.; ZHANG, J.; WANG, J. Proteomic analysis of brain proteins of rats exposed to high fluoride and low iodine. **Arch Toxicol**, 85, n. 1, p. 27-33, Jan 2011.

GRANDJEAN, P.; OLSEN, J. H.; JENSEN, O. M.; JUEL, K. Cancer incidence and mortality in workers exposed to fluoride. **J Natl Cancer Inst**, 84, n. 24, p. 1903-1909, Dec 16 1992.

GRANT, A. G.; FLOMEN, R. M.; TIZARD, M. L.; GRANT, D. A. Differential screening of a human pancreatic adenocarcinoma lambda gt11 expression library has identified increased transcription of elongation factor EF-1 alpha in tumour cells. **Int J Cancer**, 50, n. 5, p. 740-745, Mar 12 1992.

GROBER, J.; ZAGHINI, I.; FUJII, H.; JONES, S. A. *et al.* Identification of a bile acid-responsive element in the human ileal bile acid-binding protein gene. Involvement of the farnesoid X receptor/9-cis-retinoic acid receptor heterodimer. **J Biol Chem**, 274, n. 42, p. 29749-29754, Oct 15 1999.

GUYTON, A. C.; HALL, J. E. **Textbook of medical physiology**. 13 ed. Philadelphia: Elsevier Health Sciences, 2015. 1264 p.

HOFMANN, B.; HECHT, H. J.; FLOHE, L. Peroxiredoxins. **Biol Chem**, 383, n. 3-4, p. 347-364, Mar-Apr 2002.

HOLZER, P.; HOLZER-PETSCHE, U. Tachykinins in the gut. Part II. Roles in neural excitation, secretion and inflammation. **Pharmacol Ther**, 73, n. 3, p. 219-263, 1997.

HOLZER, P.; LIPPE, I. T. Substance P can contract the longitudinal muscle of the guinea-pig small intestine by releasing intracellular calcium. **Br J Pharmacol**, 82, n. 1, p. 259-267, May 1984.

HUSSAIN, J.; HUSSAIN, I.; SHARMA, K. C. Fluoride and health hazards: community perception in a fluorotic area of central Rajasthan (India): an arid environment. **Environ Monit Assess**, 162, n. 1-4, p. 1-14, Mar 2010.

IHEOZOR-EJIOFOR, Z.; WORTHINGTON, H. V.; WALSH, T.; O'MALLEY, L. *et al.* Water fluoridation for the prevention of dental caries. **Cochrane Database Syst Rev**, n. 6, p. CD010856, Jun 18 2015.

IIIZUMI, G.; SADOYA, Y.; HINO, S.; SHIBUYA, N. *et al.* Proteomic characterization of the site-dependent functional difference in the rat small intestine. **Biochim Biophys Acta**, 1774, n. 10, p. 1289-1298, Oct 2007.

INKIELEWICZ-STEPNIAK, I.; CZARNOWSKI, W. Oxidative stress parameters in rats exposed to fluoride and caffeine. **Food Chem Toxicol**, 48, n. 6, p. 1607-1611, Jun 2010.

JANKNECHT, R. Multi-talented DEAD-box proteins and potential tumor promoters: p68 RNA helicase (DDX5) and its paralog, p72 RNA helicase (DDX17). **Am J Transl Res**, 2, n. 3, p. 223-234, May 5 2010.

JUNG, D.; FANTIN, A. C.; SCHEURER, U.; FRIED, M. *et al.* Human ileal bile acid transporter gene ASBT (SLC10A2) is transactivated by the glucocorticoid receptor. **Gut**, 53, n. 1, p. 78-84, Jan 2004.

KEELY, S. J.; WALTERS, J. R. The Farnesoid X Receptor: Good for BAD. **Cell Mol Gastroenterol Hepatol**, 2, n. 6, p. 725-732, Nov 2016.

KHAN, Z. N.; SABINO, I. T.; DE SOUZA MELO, C. G.; MARTINI, T. *et al.* Liver Proteome of Mice with Distinct Genetic Susceptibilities to Fluorosis Treated with Different Concentrations of F in the Drinking Water. **Biol Trace Elem Res**, 187, n. 1, p. 107-119, Jan 2019.

KOBAYASHI, C. A.; LEITE, A. L.; PERES-BUZALAF, C.; CARVALHO, J. G. *et al.* Bone response to fluoride exposure is influenced by genetics. **PLoS One**, 9, n. 12, p. e114343, 2014.

KOBAYASHI, C. A.; LEITE, A. L.; SILVA, T. L.; SANTOS, L. D. *et al.* Proteomic analysis of kidney in rats chronically exposed to fluoride. **Chem Biol Interact**, 180, n. 2, p. 305-311, Jul 15 2009.

KRISHNAMACHARI, K. A. Skeletal fluorosis in humans: a review of recent progress in the understanding of the disease. **Prog Food Nutr Sci**, 10, n. 3-4, p. 279-314, 1986.

KRISTO, I.; BAJUSZ, I.; BAJUSZ, C.; BORKUTI, P. *et al.* Actin, actin-binding proteins, and actin-related proteins in the nucleus. **Histochem Cell Biol**, 145, n. 4, p. 373-388, Apr 2016.

LANDRIER, J. F.; ELORANTA, J. J.; VAVRICKA, S. R.; KULLAK-UBLICK, G. A. The nuclear receptor for bile acids, FXR, transactivates human organic solute transporter-alpha and -beta genes. **Am J Physiol Gastrointest Liver Physiol**, 290, n. 3, p. G476-485, Mar 2006.

LEHNINGER, A. L.; NELSON, D. L.; COX, M. M. **Lehninger principles of biochemistry**. 3. ed. ed. São Paulo: 2002.

LEITE ADE, L.; SANTIAGO, J. F., Jr.; LEVY, F. M.; MARIA, A. G. *et al.* Absence of DNA damage in multiple organs (blood, liver, kidney, thyroid gland and urinary bladder) after acute fluoride exposure in rats. **Hum Exp Toxicol**, 26, n. 5, p. 435-440, May 2007.

LIMA LEITE, A.; GUALIUME VAZ MADUREIRA LOBO, J.; BARBOSA DA SILVA PEREIRA, H. A.; SILVA FERNANDES, M. *et al.* Proteomic analysis of gastrocnemius muscle in rats with streptozotocin-induced diabetes and chronically exposed to fluoride. **PLoS One**, 9, n. 9, p. e106646, 2014.

LOBO, J. G.; LEITE, A. L.; PEREIRA, H. A.; FERNANDES, M. S. *et al.* Low-Level Fluoride Exposure Increases Insulin Sensitivity in Experimental Diabetes. **J Dent Res**, 94, n. 7, p. 990-997, Jul 2015.

LUMAN, W.; WILLIAMS, A. J.; MERRICK, M. V.; EASTWOOD, M. A. Idiopathic bile acid malabsorption: long-term outcome. **Eur J Gastroenterol Hepatol**, 7, n. 7, p. 641-645, Jul 1995.

MALI, V. R.; DESHPANDE, M.; PAN, G.; THANDAVARAYAN, R. A. *et al.* Impaired ALDH2 activity decreases the mitochondrial respiration in H9C2 cardiomyocytes. **Cell Signal**, 28, n. 2, p. 1-6, Feb 2016.

MALVEZZI, M.; PEREIRA, H.; DIONIZIO, A.; ARAUJO, T. T. *et al.* Low-level fluoride exposure reduces glycemia in NOD mice. **Ecotoxicol Environ Saf**, 168, p. 198-204, Jan 30 2019.

MARVIN-GUY, L.; LOPES, L. V.; AFFOLTER, M.; COURTET-COMPONDU, M. C. *et al.* Proteomics of the rat gut: analysis of the myenteric plexus-longitudinal muscle preparation. **Proteomics**, 5, n. 10, p. 2561-2569, Jul 2005.

MAZE, I.; NOH, K. M.; SOSHNEV, A. A.; ALLIS, C. D. Every amino acid matters: essential contributions of histone variants to mammalian development and disease. **Nat Rev Genet**, 15, n. 4, p. 259-271, Apr 2014.

MELO, C. G. d. S. **Avaliação da inervação entérica e análise proteômica do intestino delgado de ratos expostos à dose aguda ou crônica de fluoreto**. 2015. 456 f. (Doutorado) - Faculdade de Odontologia de Bauru. , Universidade de São Paulo, Bauru.

MELO, C. G. S.; PERLES, J.; ZANONI, J. N.; SOUZA, S. R. G. *et al.* Enteric innervation combined with proteomics for the evaluation of the effects of chronic fluoride exposure on the duodenum of rats. **Sci Rep**, 7, n. 1, p. 1070, Apr 21 2017.

MENG, T.; LIU, L.; HAO, R.; CHEN, S. *et al.* Transgelin-2: A potential oncogenic factor. **Tumour Biol**, 39, n. 6, p. 1010428317702650, Jun 2017.

NIU, R.; LIU, S.; WANG, J.; ZHANG, J. *et al.* Proteomic analysis of hippocampus in offspring male mice exposed to fluoride and lead. **Biol Trace Elem Res**, 162, n. 1-3, p. 227-233, Dec 2014.

NOPAKUN, J.; MESSER, H. H. Mechanism of fluoride absorption from the rat small intestine. **Nutr Res**, 10, p. 771-779, 1990.

NOPAKUN, J.; MESSER, H. H.; VOLLER, V. Fluoride absorption from the gastrointestinal tract of rats. **J Nutr**, 119, n. 10, p. 1411-1417, Oct 1989.

PEREIRA, H.; DIONIZIO, A. S.; ARAUJO, T. T.; FERNANDES, M. D. S. *et al.* Proposed mechanism for understanding the dose- and time-dependency of the effects of fluoride in the liver. **Toxicol Appl Pharmacol**, 358, p. 68-75, Nov 1 2018.

PEREIRA, H. A.; DIONIZIO, A. S.; FERNANDES, M. S.; ARAUJO, T. T. *et al.* Fluoride Intensifies Hypercaloric Diet-Induced ER Oxidative Stress and Alters Lipid Metabolism. **PLoS One**, 11, n. 6, p. e0158121, 2016.

PEREIRA, H. A.; LEITE ADE, L.; CHARONE, S.; LOBO, J. G. *et al.* Proteomic analysis of liver in rats chronically exposed to fluoride. **PLoS One**, 8, n. 9, p. e75343, 2013.

RAMESH, N.; VUAYARAGHAVAN, A. S.; DESAI, B. S.; NATARAJAN, M. *et al.* Low levels of p53 mutations in Indian patients with osteosarcoma and the correlation with fluoride levels in bone. **J Environ Pathol Toxicol Oncol**, 20, n. 3, p. 237-243, 2001.

RIBEIRO, D. A.; CARDOSO, C. M.; YUJRA, V. Q.; M, D. E. B. V. *et al.* Fluoride Induces Apoptosis in Mammalian Cells: In Vitro and In Vivo Studies. **Anticancer Res**, 37, n. 9, p. 4767-4777, Sep 2017.

RICCIO, A. Dynamic epigenetic regulation in neurons: enzymes, stimuli and signaling pathways. **Nat Neurosci**, 13, n. 11, p. 1330-1337, Nov 2010.

RIVERA, L. R.; POOLE, D. P.; THACKER, M.; FURNESS, J. B. The involvement of nitric oxide synthase neurons in enteric neuropathies. **Neurogastroenterol Motil**, 23, n. 11, p. 980-988, Nov 2011.

ROSSEL, P.; SORTSOE JENSEN, H.; QVIST, P.; ARVESCHOUG, A. Prognosis of adult-onset idiopathic bile acid malabsorption. **Scand J Gastroenterol**, 34, n. 6, p. 587-590, Jun 1999.

SANO, H.; EGUEZ, L.; TERUEL, M. N.; FUKUDA, M. *et al.* Rab10, a target of the AS160 Rab GAP, is required for insulin-stimulated translocation of GLUT4 to the adipocyte plasma membrane. **Cell Metab**, 5, n. 4, p. 293-303, Apr 2007.

SAPORITA, A. J.; CHANG, H. C.; WINKELER, C. L.; APICELLI, A. J. *et al.* RNA helicase DDX5 is a p53-independent target of ARF that participates in ribosome biogenesis. **Cancer Res**, 71, n. 21, p. 6708-6717, Nov 1 2011.

SCHAFER, K. H.; VAN GINNEKEN, C.; COPRAY, S. Plasticity and neural stem cells in the enteric nervous system. **Anat Rec (Hoboken)**, 292, n. 12, p. 1940-1952, Dec 2009.

SHANTHAKUMARI, D.; SRINIVASALU, S.; SUBRAMANIAN, S. Effect of fluoride intoxication on lipidperoxidation and antioxidant status in experimental rats. **Toxicology**, 204, n. 2-3, p. 219-228, Nov 15 2004.

SOARES, A.; BERALDI, E. J.; FERREIRA, P. E.; BAZOTTE, R. B. *et al.* Intestinal and neuronal myenteric adaptations in the small intestine induced by a high-fat diet in mice. **BMC Gastroenterol**, 15, p. 3, Jan 22 2015.

STRUNECKA, A.; PATOCKA, J.; BLAYLOCK, R.; CHINOY, N. Fluoride interactions: from molecules to disease. **Current Signal Transduction Therapy**, 2, n. 3, p. 190-213, 2007.

TANIGUCHI, T.; IIZUMI, Y.; WATANABE, M.; MASUDA, M. *et al.* Resveratrol directly targets DDX5 resulting in suppression of the mTORC1 pathway in prostate cancer. **Cell Death Dis**, 7, p. e2211, May 5 2016.

THOMPSON, C. A.; WOJTA, K.; PULAKANTI, K.; RAO, S. *et al.* GATA4 Is Sufficient to Establish Jejunal Versus Ileal Identity in the Small Intestine. **Cell Mol Gastroenterol Hepatol**, 3, n. 3, p. 422-446, May 2017.

UNIPROT, C. UniProt: a worldwide hub of protein knowledge. **Nucleic Acids Res**, 47, n. D1, p. D506-D515, Jan 8 2019.

VITERI, F. E.; SCHNEIDER, R. E. Gastrointestinal alterations in protein-calorie malnutrition. **Med Clin North Am**, 58, n. 6, p. 1487-1505, Nov 1974.

WHITFORD, G. M. Acute and Chronic Fluoride Toxicity. **Journal of Dental Research**, 71, n. 5, p. 1249-1254, May 1992.

WHITFORD, G. M. The metabolism and toxicity of fluoride. **Monogr Oral Sci**, 16 Rev 2, p. 1-153, 1996.

WHITFORD, G. M. Acute toxicity of ingested fluoride. **Monogr Oral Sci**, 22, p. 66-80, 2011.

XIONG, X.; LIU, J.; HE, W.; XIA, T. *et al.* Dose-effect relationship between drinking water fluoride levels and damage to liver and kidney functions in children. **Environ Res**, 103, n. 1, p. 112-116, Jan 2007.

XU, H.; HU, L. S.; CHANG, M.; JING, L. *et al.* Proteomic analysis of kidney in fluoride-treated rat. **Toxicol Lett**, 160, n. 1, p. 69-75, Dec 30 2005.

YAKABE, K.; MURAKAMI, A.; KAJIMURA, T.; NISHIMOTO, Y. *et al.* Functional significance of transgelin-2 in uterine cervical squamous cell carcinoma. **J Obstet Gynaecol Res**, 42, n. 5, p. 566-572, May 2016.

YAN, X.; YAN, X.; MORRISON, A.; HAN, T. *et al.* Fluoride induces apoptosis and alters collagen I expression in rat osteoblasts. **Toxicol Lett**, 200, n. 3, p. 133-138, Feb 05 2011.

YANG, L.; LIN, C.; LIU, Z. R. P68 RNA helicase mediates PDGF-induced epithelial mesenchymal transition by displacing Axin from beta-catenin. **Cell**, 127, n. 1, p. 139-155, Oct 6 2006.

ZHOU, H.; ZHANG, Y.; WU, L.; XIE, W. *et al.* Elevated transgelin/TNS1 expression is a potential biomarker in human colorectal cancer. **Oncotarget**, 9, n. 1, p. 1107-1113, Jan 2 2018.

ANNEX

ANEXO A – **APROVAÇÃO PELO COMITE DE ÉTICA**

Universidade de São Paulo
Faculdade de Odontologia de Bauru

Comissão de Ética no Ensino e Pesquisa em Animais

PROTOCOLO DE RECEBIMENTO
*Proc. N° **012/2016***

Título do Projeto de Pesquisa ou Roteiro de Aula:	*Análise proteômica do jejuno e íleo em ratos expostos a dose aguda ou crônica de fluoreto*
Pesquisador Responsável:	Marília Afonso Rabelo Buzalaf
Pesquisador Executor:	Aline Salgado Dionizio
Colaboradores:	Letícia Alves de Lima Ferrari
Data de entrega :	**25 de maio de 2016**
Reunião da CEEPA :	**17 de junho de 2016**

Maristela Petenuci Ferrari
Secretária da Comissão de Ética no Ensino e Pesquisa em Animais

Al. Dr. Octávio Pinheiro Brisolla, 9-75 – Bauru-SP – CEP 17012-101 – C.P. 73
e-mail: ceepa@fob.usp.br – Fone/FAX (0xx14) 3235-8356
http://www.fob.usp.br

ANEXO B - **CARTA DE DOAÇÃO DAS PEÇAS ANATÔMICAS**

TERMO DE DOAÇÃO DE PEÇAS ANATÔMICAS

Carina Guimaraes de Souza Melo, inscrita no CPF 304430188-20, situada(o) à Av. Affonso Jose alello, 8-200, Condominio Villaggio III casa D-19, na cidade de Bauru, estado de Sao Paulo, telefone (14) 32392569, e-mail carinamgs@yahoo.com.br, DOA, por este instrumento, a quantidade de 30 (trinta) íleo e 30 (trinta) jejuno (parte do intestino delgado) de ratos Wistar macho, obtidas no projeto de pesquisa aprovado pela CEEPA (**Proc. CEEPA nº 014/2011**), sob responsabilidade do Profa. Dra. Marília Afonso Rabelo Buzalaf, para desenvolvimento da pesquisa, intitulada *"Análise proteômica do jejuno e íleo em ratos expostos a dose aguda ou crônica de fluoreto."*, sob responsabilidade do pesquisador Profa. Dra. Marília Afonso Rabelo Buzalaf.

Bauru, 24 de Maio de 2016.

Carina Guimaraes de Souza Melo

ANEXO C – **ARTIGO PUBLICADO SCIENTIFIC REPORTS (ARTIGO 1)**

www.nature.com/scientificreports

SCIENTIFIC REPORTS

OPEN

Chronic treatment with fluoride affects the jejunum: insights from proteomics and enteric innervation analysis

Received: 7 September 2017
Accepted: 6 February 2018
Published online: 16 February 2018

Aline Salgado Dionizio[1], Carina Guimarães Souza Melo[1], Isabela Tomazini Sabino-Arias[1], Talita Mendes Silva Ventura[1], Aline Lima Leite[1], Sara Raquel Garcia Souza[2], Erika Xavier Santos[2], Alessandro Domingues Heubel[2], Juliana Gadelha Souza[1], Juliana Vanessa Colombo Martins Perles[2], Jacqueline Nelisis Zanoni[2] & Marília Afonso Rabelo Buzalaf[1]

Gastrointestinal symptoms are the first signs of fluoride (F) toxicity. In the present study, the jejunum of rats chronically exposed to F was evaluated by proteomics, as well as by morphological analysis. *Wistar* rats received water containing 0, 10 or 50 mgF/L during 30 days. HuC/D, neuronal Nitric Oxide (nNOS), Vasoactive Intestinal Peptide (VIP), Calcitonin Gene Related Peptide (CGRP), and Substance P (SP) were detected in the myenteric plexus of the jejunum by immunofluorescence. The density of nNOS-IR neurons was significantly decreased (compared to both control and 10 mgF/L groups), while the VIP-IR varicosities were significantly increased (compared to control) in the group treated with the highest F concentration. Significant morphological changes were seen observed in the density of HUC/D-IR neurons and in the area of SP-IR varicosities for F-treated groups compared to control. Changes in the abundance of various proteins correlated with relevant biological processes, such as protein synthesis, glucose homeostasis and energy metabolism were revealed by proteomics.

Fluoride (F) is considered one of the essential elements for the maintenance of the normal cellular processes in the organism[1] and is largely employed in dentistry to control dental caries[2]. However, when excessive amounts are ingested, F can induce oxidative stress and lipid peroxidation, alter intracellular homeostasis and cell cycle, disrupt communication between cells and signal transduction and induce apoptosis[3].

Nearly 25% of ingested F is absorbed from the stomach as an undissociated molecule (HF) in a process that is inversely related to pH[4], while the remainder is absorbed in the ionic form (F^-) from the small intestine, in a pH-independent manner[5]. Due to its major role in F absorption, the gastrointestinal tract (GIT) is regarded as the principal way of exposure to F[6]. Thus, gastrointestinal symptoms, including motion sickness, vomiting, diarrhea and abdominal pain are the first signs of F toxicity[7–10].

The Enteric Nervous System (ENS) is an interlinked network of neurons disposed in the intestinal walls that controls the function of the GIT[11]. Due to its control function, changes in ENS affect the absorption, secretion, permeability and motility of the GIT[12]. Recently, immunofluorescence techniques revealed important alterations in the morphology of different types of enteric neurons and proteomic analysis demonstrated changes in the expression of several proteins of the duodenum of rats[13] after chronic exposure to F, providing the first insights for the comprehension of the mechanisms underlying the actions of F on the bowel. However, the effect of F on the ENS and proteomic profile of the jejunum has never been reported. Considering that each segment of the small intestine has distinct anatomical, histological and physiological characteristics with functional implications[14], this study evaluated the morphology of distinct subtypes of enteric neurons of the jejunum after chronic exposure to F. Quantitative label-free proteomics tools were employed to evaluate the changes on the pattern of protein profile of the jejunum, after exposure to F, in attempt to provide mechanistic explanations for the effects of this ion in the intestine.

[1]Department of Biological Sciences, Bauru School of Dentistry, University of São Paulo, Bauru, Brazil. [2]Department of Morphophysiological Sciences, State University of Maringá, Maringá, Brazil. Correspondence and requests for materials should be addressed to M.A.R.B. (email: mburalaf@fob.usp.br)

Material and Methods

Animals and treatment. The Ethics Committee for Animal Experiments of Bauru Dental School, University of São Paulo approved all experimental protocols (#014/2011 and #012/2016). All experimental protocols were approved by. The assays conformed with the guidelines of the National Research Council. Eighteen adult male rats (60 days of life - *Rattus norvegicus*, Wistar type) were randomly assigned to 3 groups (n = 6/group). They remained one by one in metabolic cages, having access to water and food *ad libitum* under standard conditions of light and temperature. The animals received deionized water (0 mgF/L), 10 mgF/L and 50 mgF/L for 30 days as sodium fluoride (NaF) dissolved in deionized water, in order to simulate chronic intoxication with F. Since rodents metabolize F 5 times faster than humans, these F concentrations correspond to ~2 and 10 mg/L in the drinking water of humans[15]. After the experimental period, the animals received an intramuscular injection of anesthetic and muscle relaxant (ketamine chlorhydrate and xylazine chlorhydrate, respectively). While the rats were anesthetized, the peritoneal and thoracic cavities were exposed, and the heart was punctured for blood collection, using a heparinized syringe. Plasma was obtained by centrifugation at 800 g for 5 minutes for quantification of F, described in a previous publication[15]. After blood collection, the jejunum was collected for histological, immunofluorescence and proteomic analysis. For the collection of the jejunum, animal chow was removed from the animals 18 hours prior the euthanasia to decrease the volume of fecal material inside the small intestine, facilitating the cleaning process for posterior processing. After laparotomy, to remove the jejunum, initially the small intestine was localized, and the jejunum proximal limit was identified by the portion after the duodenojejunal flexure that is attached to the posterior abdominal wall by the ligament of Treitz. After incisions in the flexure and ligament, 20 centimeters distally to the incision were despised and then 15 centimeters of the jejunum were harvested for processing. After harvesting, the jejunum was washed with PBS solution applied several times with a syringe in the lumen to remove completely any residue of fecal material.

Histological analysis. This analysis was performed exactly as described by Melo, *et al.*[13].

Myenteric plexus immunohistochemistry, morphometric and semi-quantitative analysis. These analyses were performed exactly as described by Melo, *et al.*[13].

Proteomic analysis. The frozen jejunum was homogenized in a cryogenic mill (model 6770, SPEX, Metuchen, NJ, EUA). Samples from 2 animals were pooled and analyses were carried out in triplicates. Protein extraction was performed by incubation in lysis buffer (7 M urea, 2 M thiourea, 40 mM DTT, all diluted in AMBIC solution) under constant stirring at 4 °C. Samples were centrifuged at 14000 rpm for 30 min at 4 °C and the supernatant was collected. Protein quantification was performed[16]. To 50 µL of each sample (containing 50 µg protein) 25 µL of 0.2% Rapigest (WATERS cat# 186001861) was added, followed by agitation and then 10 µL 50 mM AMBIC were added. Samples were incubated for 30 min at 37 °C. Samples were reduced (2.5 µL 100 mM DTT; BIORAD, cat# 161–0611) and alkylated (2.5 µL 300 mM IAA; GE, cat# RPN 6302 V) under dark at room temperature for 30 min. Digestion was performed at 37 °C overnight by adding 100 ng trypsin (PROMEGA, cat #V5280). After digestion, 10 µL of 5% TFA were added, incubated for 90 min at 37 °C and sample was centrifuged (14000 rpm at 6 °C for 30 min). Supernatant was purified using C 18 Spin columns (PIERCE, cat #89870). Samples were resuspended in 200 µL 3% acetonitrile.

LC-MS/MS and bioinformatics analyses. The peptides identification was done on a nanoAcquity UPLC-Xevo QTof MS system (WATERS, Manchester, UK), using the PLGS software, as previously described[17]. Difference in abundance among the groups was obtained using the Monte-Carlo algorithm in the ProteinLynx Global Server (PLGS) software and displayed as $p < 0.05$ for down-regulated proteins and $1 - p > 0.95$ for up-regulated proteins. Bioinformatics analysis was done to compare the treated groups with the control group (Tables S1–S5), as previously reported[17–20]. The software CYTOSCAPE 3.0.4 (JAVA) was used to build networks of molecular interaction between the identified proteins, with the aid of ClueGo and ClusterMarker applications.

Results

Morphological analysis of the jejunum wall thickness. The mean (±SD) thickness of the jejunum tunica muscularis was significantly higher in the 50 mgF/L ($93.0 \pm 1.4\,\mu m^2$) when compared to control ($81.5 \pm 1.1\,\mu m^2$) and 10 mgF/L ($84.2 \pm 2.5\,\mu m^2$) groups (Bonferroni's test, $p < 0.05$). The total thickness of the jejunum wall was significantly lower in the 50 mgF/L ($742.25 \pm 7.8\,\mu m^2$) and 10 mgF/L ($734.4 \pm 11.8\,\mu m^2$) when compared to control ($783.15 \pm 5.8\,\mu m^2$) (Bonferroni's test, $p < 0.05$).

Myenteric HuC/D – IR neurons analysis. When the general population of neuron was morphometrically analyzed, the cell bodies areas (μm^2) of the HuC/D–IR neurons were not significantly different among the groups ($p > 0.05$). In the semi-quantitative analyses (neurons/cm^2), a significant decrease in the density was observed in the treated groups when compared with control ($p < 0.05$) (Table 1).

Myenteric nNOS –IR neurons analysis. The cell bodies areas (μm^2) of the nNOS-IR neurons did not present a significant difference among the groups ($p > 0.05$) in the morphometric analysis. As for the semi-quantitative analyses, a decrease in the mean value of the density for the group treated with 50 mgF/L when compared with the other groups was observed ($p < 0.05$; Table 1).

Myenteric varicosities VIP-IR, CGRP-IR or SP-IR morphometric analysis. A significant increase in the VIP-IR varicosity areas (μm^2) was detected in the group treated with 50 mgF/L when compared with the control group ($p < 0.05$). For the CGRP-IR varicosity areas, the groups did not differ significantly ($p > 0.05$). However, SP-IP varicosity areas were significantly increased in the treated groups when compared with control.

ANALYSIS	Control	10 mgF/L	50 mgF/L
Cell bodies areas of the HuC/D-IR neurons (μm^2)	304.9 ± 3.5[a]	310.7 ± 3.8[a]	304.8 ± 3.8[a]
Density HuC/D-IR neurons (neurons/cm^2)	16,968 ± 350[a]	15,420 ± 392[b]	15,250 ± 380[b]
Cell bodies areas of the nNOS-IR neurons (μm^2)	291.4 ± 3.2[a]	296.6 ± 3.5[a]	289.6 ± 2.9[a]
Density nNOS-IR neurons (neurons/cm^2)	5,725 ± 123[a]	5,559 ± 134[a]	5,176 ± 146[b]
Area VIP-IR varicosities (μm^2)	3.68 ± 0.52[a]	3.98 ± 0.03[a]	4.46 ± 0.04[b]
Area CGRP-IR varicosities (μm^2)	3.31 ± 0.03[a]	3.35 ± 0.04[a]	3.38 ± 0.03[a]
Area SP-IR varicosities (μm^2)	2.81 ± 0.01[a]	4.86 ± 0.03[b]	4.64 ± 0.03[c]

Table 1. Means and standard errors of the values of the cell bodies areas and density of HUC/D-IR and nNOS-IR neurons and VIP-IR, CGRP-IR, and SP-IR values of myenteric neurons varicosities areas of the jejunum of rats chronically exposed or not to fluoride in the drinking water. Means followed by different letters in the same line are significantly different according to Fisher's test (density HuC/D-IR and nNOS-IR neurons) or Tukey's test (other variables). $p < 0.05$. $n = 6$.

In addition, the group treated with 10mgF/L presented an area significantly higher than the group treated with 50 mgF/L (Table 1).

Typical images of the immunofluorescences are shown in Figs 1 and 2.

Proteomic analysis of the jejunum. The total numbers of proteins identified in the control, 10 and 50 mgF/L groups were 294, 343 and 322, respectively. These proteins were present in the 3 pooled samples for each group. Among them, 81 (Table S1), 120 (Table S2) and 99 (Table S3) proteins were uniquely identified in the control, 10 mgF/L and 50 mgF/L groups, respectively. In the quantitative analysis of the 10 mgF/L *vs.* control group, 30 proteins with change in expression were detected (Table S4). As for the comparison 50 mgF/L *vs.* control group, 40 proteins with change in expression were found (Table S5). Most of the proteins with changed expression were upregulated in the groups treated with F when compared with the control group (21 and 23 proteins in the groups treated with 10 mgF/L and 50 mgF/L, Tables S4 and S5, respectively).

Figures 3 and 4 show the functional classification according to the biological process with the most significant term, for the comparisons 10 mgF/L *vs.* control and 50 mgF/L *vs.* control, respectively. The group exposed to the highest F concentration had the largest alteration, with change in 15 functional categories (Fig. 4). Among them, the categories with the highest percentage of associated genes were: Cellular respiration (14.3%), NAD metabolic process (10.2%), Oxygen transport (10.2%), Chromatin silencing (8.2%) and ER-associated ubiquitin-dependent protein catabolic process (8.2%). Exposure to the lowest F concentration influenced 12 functional categories (Fig. 3). The biological processes with the highest percentage of affected genes were: Nicotinamide nucleotide metabolic process (25%), Regulation of neuronal synaptic plasticity (11.4%), NAD metabolic process (15.9%) and Positive regulation of response to wounding (9.1%). It should be highlighted that Regulation of oxidative stress-induced intrinsic apoptotic signaling pathway was also identified, with 4.5% of affected genes (4.5%).

Figures 5 and 6 show the subnetworks created by CLUSTERMARK for the comparisons 10 mgF/L *vs.* control and 50 mgF/L *vs.* control, respectively. For the 10 mgF/L group (Fig. 5), most of the proteins with change in expression interacted with *Solute carrier family 2, facilitated glucose transporter member 4* (GLUT4; P19357) and *Small ubiquitin-related modifier 3* (Q5XIF4) (Fig. 5A) or with *Polyubiquitin-C* (Q63429) and *Elongation factor 2* (P05197) (Fig. 5B). As for the group treated with 50 mgF/L, most of the proteins with change in expression interacted with GLUT4 (P19357) and *Mitogen-activated protein kinase 3* (MAPK3; P21708) (Fig. 6A) or *Polyubiquitin-C* (Q63429) (Fig. 6B).

Discussion

The small intestine is responsible for absorption of around 70–75% of F[1,21]. As consequence, gastrointestinal symptoms, such as abdominal pain, nausea, vomiting and diarrhea, are the most common occurrence in cases of excessive ingestion of F[22–25]. The mechanisms underlying these changes remain to be determined. Recently, our group took advantage of immunofluorescence and proteomics techniques to evaluate changes in the duodenum of rats after chronic exposure to F[13]. The group treated with 50 mgF/L had a significant decrease in the density of nNOS-IR neurons. Additionally, important morphological changes were seen in HUC/D-IR and nNOS-IR neurons, as well as in VIP-IR, CGRP-IR, and SP-IR varicosities for the groups treated with both 10 and 50 mgF/L. Moreover, profound proteomic alterations were observed in both treated groups. In the group treated with 10 mgF/L, most of the proteins with altered expression were upregulated. On the other hand, downregulation of several proteins was found in the group treated with the highest F concentration[13].

Many proteins observed in the previous study were correlated with the neurotransmission process, which is essential for the function of the GIT through ENS control. For example, the pattern of intestinal smooth muscle contraction can be modified when the release of neurotransmitters stimulating muscle contraction, such as SP[26] is increased or when the release of neurotransmitters promoting muscle relaxation, such as NO[27], is decreased. In the present study, both conditions might have occurred, because we found a significance increase and decrease in the mean values of the SP varicosities area and the density of nNOS-IR neurons, respectively (Table 1), which is in accordance with our previous findings for the duodenum[13]. This finding can be also associated with the significant decrease in the density of HUC/D-IR neurons (Table 1), and it could contribute to the intestinal discomfort and symptoms, such as abdominal pain and diarrhea, observed upon excessive exposure to F.

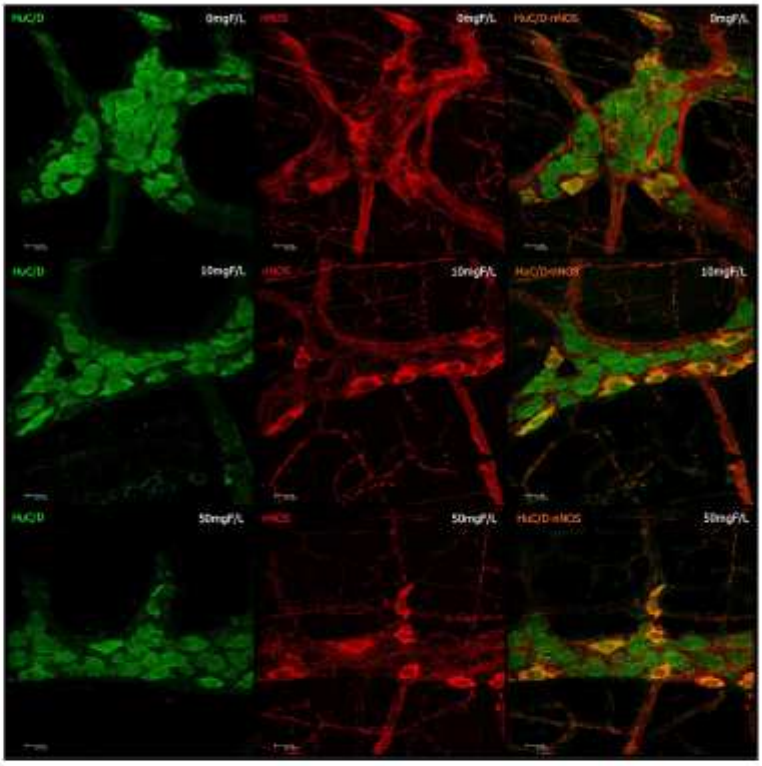

Figure 1. Photomicrography of myenteric neurons of the rats jejunum stained for HuC/D (green), nNOS (red), and double-labeling (HuC/D and nNOS) for the control group (0 mgF/L) and for the groups treated with 10 and 50 mgF/L. 20x Objective.

Another important neurotransmitter that also participates in the control of intestinal motility is VIP. In our study, it was observed a statistically significant increase in the mean value of the areas of VIP-IR myenteric varicosities in the 50 mgF/L group when compared with control. This finding is similar to what was observed in our previous study where duodenum was analyzed[13] and confirms that this dose of F can compromise the vipergic innervation of the small intestine. For the inhibitory control of motility, the main neurotransmitters involved are NO and VIP[28], so basically any changes in the vipergic innervation can alter the intestinal motility, leading to a decrease in the tone of the intestinal smooth muscle, which could trigger diarrhea or even increased susceptibility to intestinal infections by decreased intestinal transit[29]. We can also suggest, in this case, that this increase may mean upregulation in the expression of the VIP, as a response to F toxicity since other processes such as axotomy and blocking of axonal transport or hypertrophic alterations promote upregulation of VIP in enteric neurons[30]. This increase can also be related to a neuroprotective role of VIP, because it acts as a potent anti-inflammatory molecule and presents an important antioxidant activity[31–33]. In addition to this, VIP is one of the most important elements involved in enteric neuroplasticity[33], which is the ENS ability to adapt to any change in its microenvironment[34]. Due to the morphological changes that we observed in our study in the vipergic varicosities, we can suggest that F can induce important neuroplastic changes in the GIT.

Since alterations in the morphology of the intestinal wall infer important pathophysiological processes, we analyzed the total thickness of the intestinal wall, as well as the tunica muscularis separately. The group treated with 50 mgF/L presented a significant decrease in the total thickness of the intestinal wall and an increase in the thickness of the *tunica muscularis*, indicating that F can alter morphologically the jejunum wall. The finding for the *tunica muscularis* of the jejunum is in-line with our previous findings for the duodenum[13], despite the total thickness of the duodenum wall was not altered. Changes in the number and morphology of myenteric cell bodies may be related to variations of the *tunica muscularis* thickness, which presents the structures responsible for the

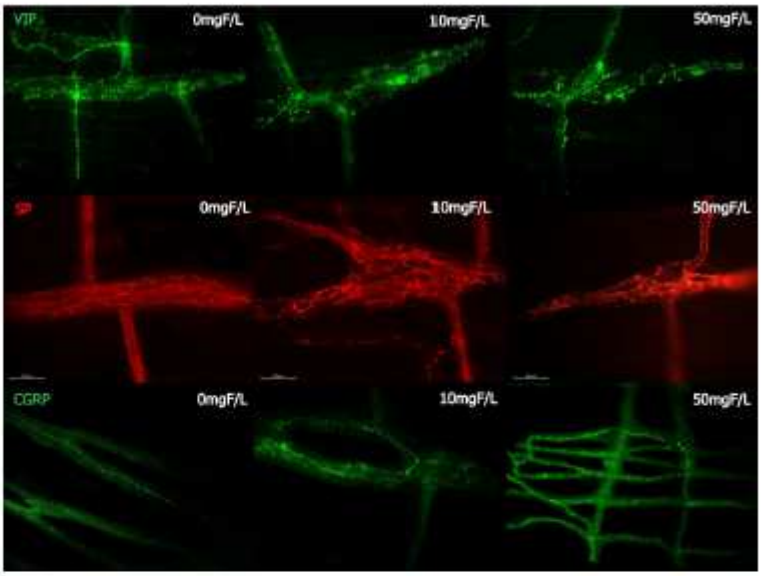

Figure 2. Photomicrography of myenteric varicosities of the rats jejunum after F chronic exposure (0, 10 or 50 mgF/L) for VIP-IR, SP-IR CGRP-IR. 40x Objective.

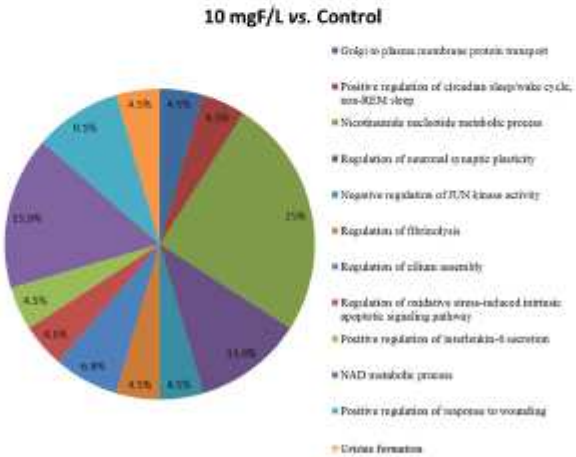

Figure 3. Functional distribution of proteins identified with differential expression in the jejunum of rats exposed to the chronic dose of 10 mgF/L vs. Control Group (0 mgF/L). Categories of proteins based on GO annotation Biological Process. Terms significant (Kappa = 0.04) and distribution according to percentage of number of genes association. Proteins access number was provided by UNIPROT. The gene ontology was evaluated according to ClueGo® pluggins of Cytoscape® software 3.4.0[49,50].

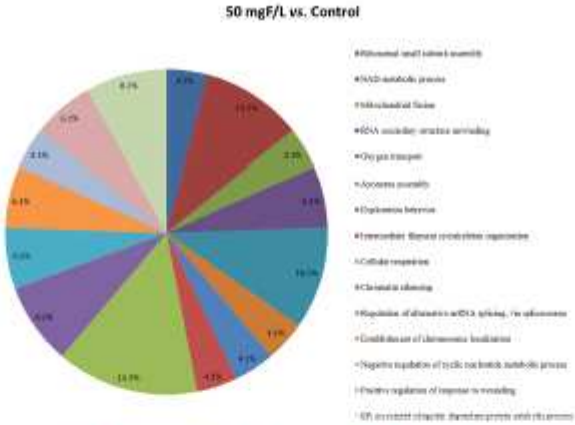

Figure 4. Functional distribution of proteins identified with differential expression in the jejunum of rats exposed to the chronic dose of 50 mgF/L *vs.* Control Group (0 mgF/L). Categories of proteins based on GO annotation Biological Process. Terms significant (Kappa = 0.04) and distribution according to percentage of number of genes association. Proteins access number was provided by UNIPROT. The gene ontology was evaluated according to ClueGo® pluggins of Cytoscape® software 3.4.0[89,90].

maintenance, development and plasticity of these neurons[31]. Similar increase in the thickness of the intestinal wall and *tunica muscularis* have been reported in the duodenum and jejunum of rats fed with a high fat diet for 8 weeks, where morphological alterations in the general population of enteric neurons and in the nitrergic population were also detected[30], emphasizing that intestinal physiology comprises many interconnected mechanisms.

As in our study F caused morphological alterations in different enteric neuronal subtypes, which present several neurotransmitters involved in the GIT motility, it is possible that these alterations affect the GIT function, and promote the important symptomatology of F toxicity on the GIT, such as abdominal pain and diarrhea. We also believe that our results are quite relevant regarding the ENS, since mechanisms of neurodegeneration associated to enteric neuropathies are characterized basically by alterations, damage or loss of enteric neurons, as observed in several important pathologies[37] and also in our study. Thus, in order to better investigate these findings involving the enteric innervation, we performed the proteomic analysis.

The proteomic approach revealed for both F doses that the majority of the proteins presenting changed expression interacted with *Solute carrier family 2, facilitated glucose transporter member 4* (GLUT4) (P19357) and *Polyubiquitin C* (Q63429). In the network comparing 10 mgF/L *vs.* control groups, 17 members of the Ras-related Rab proteins (isoforms 1A, 1B, 3A, 3C, 3D, 4A, 4B, 5A, 8A, 8B, 10, 12, 14, 26, 35, 37, and 43) were uniquely found in the group treated with 10 mgF/L (Table S2), despite some not being present in the network. The GTPases Rab proteins are known as key regulators of intracellular membrane trafficking, from the formation of transport vesicles to their fusion with membranes. Rabs modulate between an inactive form (GDP-bound) and an active form (GTP-bound). The latter can attract to membranes distinct downstream effectors that will lead to vesicle formation, movement, tethering and fusion (UNIPROT). Generally, many studies report Rab proteins as molecules present in the CNS and their specific roles. Although marked differences distinguish the neuronal function between the ENS and CNS, their similarities allow the use of some principles established for the brain environment to be reapplied in the enteric context[38]. Several cellular processes can be altered and promote the enteric neuronal alterations caused by F effects through mechanisms involving the Rab proteins, which are considered neuronal regulators involved in the traffic and signaling of different molecules that promote neurons homeostasis, such as the neurotrophins family of growth factors. The neurotrophins-receptors complexes trigger important signaling pathways that promote development, survival and other neuronal functions through intracellular transport mechanisms mediate by the Rab proteins[39].

Rab 1A is a regulator of specific vesicular trafficking from the ER to Golgi complex, and in dopaminergic neurons its expression presents a protective effect enhancing the control of motor function in surviving neurons of hemiparkinsonian animals[40]. From the family of the Rab 3 proteins, 3 members were present in the 10 mgF/L group, Rab 3A, Rab 3C, and Rab 3D. The Rab 3 family is observed in different cell types with high exocytic function[41], in which they function as exocytosis regulators[42] correlated with neuronal traffic[39], and are present in synaptic vesicles, modulating the neurotransmitter release[42]. Rab 3A is the most abundant isoform in the brain, where it presents a modulatory function in synaptic membrane fusion through a Ca^{2+}-dependent manner[43]. In the peripheral nervous system Rab 3A has increased expression in sciatic nerve lesion area associated to an increase in the expression of two other important proteins that contribute to neurotransmission, synaptophysin and synapsin I[44]. Rab 3C is highly expressed in primary hippocampal neurons, mediating regulated exocytosis[45],

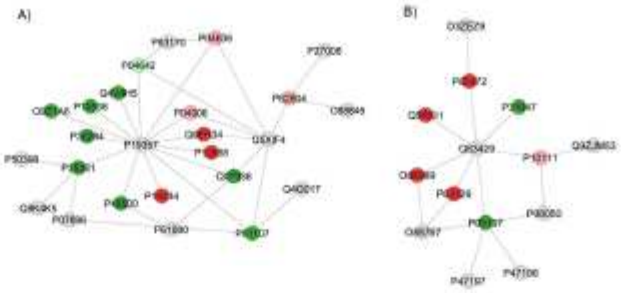

Figure 5. Subnetworks created by ClusterMark® to establish the interaction between proteins identified with differential expression in the 10 mgF/L group in relation to the control group. The color of the nodes indicates the differential expression of the respective named protein with its access code. The dark red and dark green nodes indicate proteins unique to the control and 10 mgF/L groups, respectively. The nodes in gray indicate the interaction proteins that are offered by CYTOSCAPE®, which were not identified in the present study and the light red and light green nodes indicate downregulation and upregulation, respectively. In (**A**), the access numbers in the gray nodes correspond to: *Dynein light chain 1, cytoplasmic* (P63170), *Poly [ADP-ribose] polymerase 1* (P27008), *E3 ubiquitin-protein ligase RNF4* (O88846), *Small ubiquitin-related modifier 3* (Q5XIF4), *Nischarin* (Q4G017), *Heterogeneous nuclear ribonucleoprotein K* (P61980), *Peroxisomal bifunctional enzyme* (P07896), *Lethal(2) giant larvae protein homolog 1* (Q8K4K5), *Rab GDP dissociation inhibitor alpha* (P50398) and *Solute carrier family 2, facilitated glucose transporter member 4* (P19357). The access numbers of the unique proteins of the control (dark red nodes) correspond to: *Aconitate hydratase, mitochondrial* (Q9ER34), *Cytochrome c oxidase subunit 4 isoform 1, mitochondrial* (P10888) and *NADH dehydrogenase [ubiquinone] flavoprotein 2, mitochondrial* (P19234). The accession numbers of the unique 10 mgF/L (dark green nodes) proteins correspond to: *Aspartyl aminopeptidase* (Q4V8H5), *Ras-related protein Rab-1B* (P10536), *Vigilin* (Q9Z1A6), *Ras-related protein Rab-12* (P35284), *Ras-related protein Rab-10* (P35281), *Triosephosphate isomerase* (P48500), *Annexin A2* (Q07936) and *Ras-related protein Rab-14* (P61107). The access numbers of the downregulated proteins (light red nodes) correspond to: *Malate dehydrogenase, mitochondrial* (P04636), *Glutathione S-transferase P* (P04906) and *Histone H4* (P62804). The accession numbers of the upregulated proteins (light green nodes) correspond to: *L-lactate dehydrogenase A chain* (P04642). In (**B**), the access numbers in the gray nodes correspond to: *Protein Syd* (D3ZEZ9), *Polyubiquitin-C* (Q63429), *Apoptosis-inducing factor 1, mitochondrial* (Q9JM53), *Protein deglycase DJ-1* (O88767), *RAC-beta serine/threonine-protein kinase* (P47197), *RAC-alpha serine/threonine-protein kinase* (P47196) and *Gap junction alpha-1 protein* (P08050). The access numbers of the unique proteins of the control (dark red nodes) correspond to: *Vinculin* (P85972), *Eukaryotic initiation factor 4A-II* (Q5RKI1), *Malate dehydrogenase, cytoplasmic* (O88989) and *40S ribosomal protein S10* (P63326). The accession numbers of the single 10 mgF/L (dark green nodes) proteins correspond to: *Elongation factor 2* (P05197) and *Sodium- and chloride-dependent GABA transporter 3* (P31647). The access numbers of the downregulated proteins (light red nodes) correspond to: *Peptidyl-prolyl cis-trans isomerase A* (P10111).

while Rab 3D is present in secretory granules and vesicles of other cell types, such as adipocytes, exocrine glands, hematopoietic cells[46], and low levels of expression were already identified in the duodenum, confirming its presence in exocrine cells of the GIT[47].

The Rabs 4A and 4B were also identified as exclusive for the 10 mgF/L, and Rab4 is described as a regulator of early endosomes in the synapses, contributing to neurotransmitter receptor recycling through endosomes acting associated to other molecules in the later steps of the endocytic recycling pathway in dendrites, directing the neuronal membrane receptor trafficking[48]. This process is extremely important for the delivery of neurotransmitter receptors into the synaptic membrane, determining the synaptic function and plasticity. Rab 5A presents a role in axonal and dendritic endocytosis, contributing to the biogenesis of synaptic vesicles[49]. Rab 8 presents the same role as Rab 4, being required to direct into synapses neurotransmitter receptors as the AMPA-type glutamatergic receptors, presenting an important role in the control of synaptic function and plasticity at the postsynaptic membrane[50].

Rab 10 is required for the secretion of neuropeptides through the release of dense core vesicles, which is a mechanism that modulates neuronal activity[51]. It is also a regulator of membrane trafficking during dendrite morphogenesis, and loss of RAB 10 decreases proximal dendritic arborization in the multi-dendritic PVD neurons[52]. In the CNS Rab 12 is colocalized with M98K, and overexpression of the latter induces cell death in retinal glial cells, while knockdown of Rab 12 reduces M98K-induced cell death in the same cells through the autophagy mechanism[53].

Rab 26 promotes in the brain the formation of clusters of vesicles in neuritis[54], and the authors suggest a new mechanism for degradation of synaptic vesicles in which Rab 26 selectively conducts synaptic and secretory

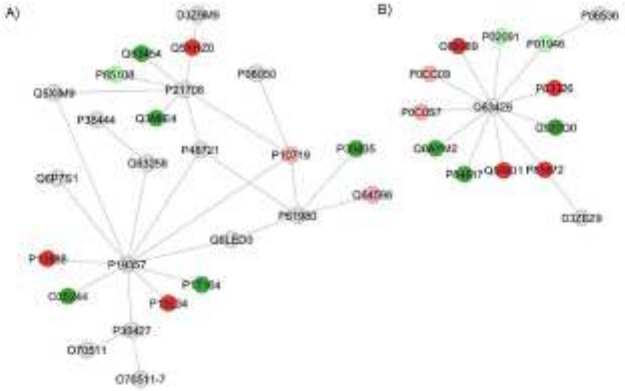

Figure 6. Subnetworks created by ClusterMark® to establish the interaction between proteins identified with differential expression in the 50 mgF/L group in relation to the control group. The color of the nodes indicates the differential expression of the respective named protein with its access code. The dark red and dark green nodes indicate proteins unique to the control and 50 mgF/L groups, respectively. The nodes in gray indicate the interaction proteins that are offered by CYTOSCAPE®, which were not identified in the present study and the light red and light green nodes indicate downregulation and upregulation, respectively. In (**A**), the access numbers in the gray nodes correspond to: *PTEN induced putative kinase 1 (Predicted)* (D3Z9M9), *Mitogen-activated protein kinase 3* (P21708), *T-complex protein 1 subunit beta* (Q5XIM9), *Gap junction alpha-1 protein* (P08050), *Cartilage oligomeric matrix protein* (P35444), *Acid ceramidase* (Q6P7S1), *Integrin alpha-7* (Q63258), *Stress-70 protein, mitochondrial* (P48721), *Solute carrier family 2, facilitated glucose transporter member 4* (P19357), *Histone H3.1* (Q6LED0), *Heterogeneous nuclear ribonucleoprotein K* (P61980), *Ankyrin-3* (O70511), *Plectin* (P30427) and *Ankyrin-3* (O70511-7). The access numbers of the unique proteins of the control (dark red nodes) correspond to: *Malate dehydrogenase, cytoplasmic* (O88989), *40S ribosomal protein S10* (P63326), *Eukaryotic initiation factor 4A-II* (Q5RKI1) and *Vinculin* (P85972). The accession numbers of the unique 50 mgF/L (dark green nodes) proteins correspond to: *Tektin-2* (Q6AYM2), *Mitochondrial fission 1 protein* (P84817) and *Paralemmin-1* (Q920Q0). The access numbers of the downregulated proteins (light red nodes) correspond to: *Histone H2A type 2-A* (P0CC09) and *Histone H2A.Z* (P0C0S7). The accession numbers of the upregulated proteins (light green nodes) correspond to: *Hemoglobin subunit beta-1* (P02091) and *Hemoglobin subunit alpha-1/2* (P01946). In (**B**), the access numbers in the gray nodes correspond to: *Polyubiquitin-C (Q63429), Protein Svil (D3ZEZ9) e Glucocorticoid receptor (P06536).* The access numbers of the unique proteins of the control (dark red nodes) correspond to: *Heat shock protein 75 kDa, mitochondrial* (Q5XHZ0), *Cytochrome c oxidase subunit 4 isoform 1, mitochondrial* (P10888) and *NADH dehydrogenase [ubiquinone] flavoprotein 2, mitochondrial* (P19234). The accession numbers of the single 50 mgF/L (dark green nodes) proteins correspond to: *Mitogen-activated protein kinase 4* (Q63454), *Synaptic vesicle membrane protein VAT-1 homolog* (Q3MIE4), *ATP-dependent 6-phosphofructokinase, liver type* (P30835), *Tissue alpha-L-fucosidase* (P17164) and *Peroxiredoxin-6* (O35244). The access numbers of the downregulated proteins (light red nodes) correspond to: *ATP synthase subunit beta, mitochondrial* (P10719) and *e Histone H2A type 1-F* (Q64598). The accession numbers of the upregulated proteins (light green nodes) correspond to: *Tubulin beta-2A chain* (P85108).

vesicles into preautophagosomal structures. In neuronal immortalized cells, Rab 35 promotes neurite differentiation and favors axon elongation in rat primary neurons in an activity-dependent manner[55].

The fact that several members of the Rab proteins were expressed exclusively in the 10 mgF/L group might indicate that this F concentration could affect the neuronal functions, since different Rab proteins regulate distinct processes in the neuronal environment. Since the 10 mgF/L concentration caused a decrease in the enteric neuronal density, which can compromise the enteric neuronal activity, the expression of several Rab proteins can reflect an attempt to keep the neurotransmission unaltered in the presence of F. Besides the neuronal activity, other important biological mechanisms involve the Rab proteins action. In the network comparing 10 mgF/L *vs.* control groups, the isoforms 1B, 10, 12 and 14 interact with GLUT4, and especially Rab 10 and Rab 14, are required in GLUT4 translocation to the plasma membrane[56,57]. Their increased expression might help to explain the increased sensitivity to insulin recently reported to occur in rats with diabetes induced by streptozotocin exposed to 10 mgF/L in the drinking water[58]. The increased expression of Rab 10 and Rab 14 might facilitate glucose uptake. Rab 37 and Rab 3A, also present among the proteins exclusively expressed in the 10 mgF/L group, are involved in the insulin release. Rab 3A has an important role in the hormone release from pancreatic β-cells with a regulatory control on insulin-containing secretion[59]. Rab 37, with a high sequence homology with Rab 3A, has also been reported to participate in regulated secretion in mammalian cells in the control of insulin exocytosis

through a different mechanism of Rab 3A[60]. According to the authors, impairment of Rab 37 expression may contribute to abnormal insulin release in pre-diabetic and diabetic conditions. We can infer that the expression of both proteins indicates that the insulin release mechanism could be altered with this F dose. We also observed an increase in *L-lactate dehydrogenase A chain* (LDH) (P04642) upon exposure to 10 mgF/L. This enzyme converts pyruvate to lactate with regeneration of NADH into NAD^+. It is an alternative way to supply the lack of oxygen for aerobic oxidation of pyruvate and NADH produced in glycolysis[61]. In fact, the categories nicotinamide nucleotide metabolic process and NAD metabolic process were among the ones with the highest percentage of affected genes when the 10 mgF/L group was compared with control. Previous studies have reported increase in the LDH activity in the serum of infants who consumed water containing more than 2 mgF/L[62]. It was also overexpressed in the brain of rats treated with F[63]. When pyruvate is converted into lactate by LDH, less pyruvate is available to enter into the mitochondria and form acetyl-CoA, which is consistent with the reduction of *Malate dehydrogenase, mitochondrial* (P04636) and of enzymes related to the oxidative phosphorylation, such as *Cytochrome c oxidase subunit 4 isoform 1, mitochondrial* (P10888) and *NADH dehydrogenase [ubiquinone] flavoprotein 2, mitochondrial* (P19234). According to Barbier, *et al.*[3], F has an inhibitory effect on the activity of citric acid cycle enzymes, in agreement with our finding of reduction in *Malate dehydrogenase, mitochondrial*. Another protein with altered expression (downregulation) in the group treated with 10 mgF/L that interacts with GLUT4 was *Glutathione S-transferase P* (P04906) that was also found downregulated in the duodenum of rats treated with the same dose of F[13]. This enzyme is involved in the metabolism and detoxification of xenobiotics[64]. Many proteins with altered expression in the network comparing 10 mgF/L *vs.* control groups interact with *Polyubiquitin C* (Q63429), a highly conserved polypeptide that is covalently bound to other cellular proteins to signal processes such as protein degradation, protein/protein interaction and protein intracellular trafficking[65]. Among them are proteins related to translation, that were absent in the group treated with 10 mgF/L, such as *Eukaryotic initiation factor 4A-II* (Q5RKI1) and *40 S ribosomal protein S10* (P63326). The latter was also reduced in the group treated with 50 mgF/L both in the present study and in a previous study where duodenum was analyzed[13]. In addition, *Peptidyl-prolyl cis-trans isomerase A* (P10111) was reduced in the group treated with 10 mgF/L compared to control, which might impair protein folding. Also involved in protein synthesis, *Elongation factor 2* (P05197) presented altered expression upon exposure to 10 mgF/L. This protein was present only in the group treated with 10 mgF/L, and catalyzes the GTP-dependent ribosomal translocation step during translation elongation (UNIPROT). Differences in expression of all these proteins indicate alterations in distinct steps of protein synthesis upon exposure to 10 mgF/L. Changes in protein synthesis might help to explain the alterations in the thickness of the jejunum wall observed in this group. Interestingly, *Elongation factor 2* interacted with two of the 3 isoforms of the protein kinase AKT, namely *RAC-alpha serine/threonine-protein kinase* (AKT1; P47196) and *RAC-beta serine/threonine-protein kinase* (AKT2; P47197) that mediate protein synthesis and glucose metabolism[66].

In the network comparing the 50 mgF/L *vs.* control groups (Fig. 6), some proteins with relevance for the neuronal homeostasis were expressed uniquely in the 50 mgF/L, such as *Tektin-2* (Q6AYM2), *Perforin-1* (Q5FVS5), and *Mitochondrial fission 1 protein* (*Fis1*-P84817). The Tektins family has significant expression in adult brain and in embryonic stages of the choroid plexus, the forming retina, and olfactory receptor neurons, and can be considered a molecular target for the comprehension of neural development[67]. Although not present in the subnetwork, Perforin participates in the $CD8^+$ T cells response, promoting granule cytotoxicity leading to a fast cellular necrosis of the target cell in minutes[68] or apoptosis in a period of hours through a mechanism in which the target cell collaborates with perforin to deliver granzymes into the cytosol[69]. Using these mechanisms perforin-dependent, $CD8^+$ T cells promote neuronal damage in inflammatory CNS disorders[70].

Mitochondrial fission is implicated in the cell death through a pathway that involves caspase activation[71], and *Mitochondrial fission 1 protein* (Fis1) is considered essential for mitochondrial fission[72]. Overexpression of Fis1 caused increase of mitochondrial fragmentation, which conducted to apoptosis or triggered autophagy[71,74], and neuroprotective effects are correlated with inhibition of Fis1[75].

The fact that these proteins presented increased expression in relation to the control group can reflect F neurotoxicity on the ENS with the concentration of 50 mgF/L, and could result in the decrease in the density of the general population of neurons since these 3 proteins are involved in pathways that conduct to cell death by distinct mechanisms.

Other proteins with altered expression interacted mainly with GLUT4 (P19357) and *Polyubiquitin C* (Q63429), which was also observed for the network comparing the 10 mgF/L *vs.* control groups (Fig. 5). In addition, *Mitogen-activated protein kinase 3* (MAPK3; P21708) was also an interacting partner as in the duodenum of rats treated with the same concentration of F in the drinking water[13]. Among the proteins that interacted with GLUT4, *Peroxiredoxin-6* (O35244) was present only in the group treated with 50 mgF/L, when compared with control (Fig. 6). This enzyme, located in the cytoplasm, protects cells against oxidative stress, in addition to modulating intracellular signaling pathways. Peroxiredoxins catalyze the reduction of H_2O_2 and hydroxyperoxide in water and alcohol[76]. Thus, changes in these proteins expression could be linked to fluoride-induced oxidative stress that has been extensively described in the literature[1,77–81]. In the group treated with 50 mgF/L, there was a remarkable downregulation in several isoforms of Histones, in comparison with control (Fig. 6 and Table S5). The major role described for histones is DNA "packaging", however, it is also well described that these proteins confer variations in chromatin structure to ensure dynamic processes of transcriptional regulation in eukaryotes[82]. Epigenetic modifications of DNA and histones are fundamental mechanisms by which neurons adapt their transcriptional response to developmental and environmental factors. Modifications in the chromatin of neurons contribute dramatically to changes in the neuronal circuits, and it is possible that histone activity is involved in disorders that compromise neuronal function[83]. Thus, changes in the expression of histones might have contributed to the alterations found in the morphology of enteric neurons in response to F exposure. In addition, structural muscle proteins such as different isoforms of actin and myosin were increased or exclusive

in the group treated with 50 mgF/L (Tables S3 and S5), which helps to explain the increase in the thickness of the jejunum *tunica muscularis*.

Probably the most remarkable finding of the present study was that when the groups treated with 10 and 50 mgF/L are compared with control, some proteins related to energetic metabolism presented similar alterations in expression, regardless the dose of F, such as: *Cytochrome c oxidase subunit 4 isoform 1, mitochondrial* (P10888), *NADH dehydrogenase [ubiquinone] flavoprotein 2, mitochondrial* (P19234), *Malate dehydrogenase, mitochondrial* (P04636), *Malate dehydrogenase, cytoplasmic* (O88989) and *L-lactate dehydrogenase A chain* (P04642). The absence of *Malate dehydrogenase, mitochondrial* (P04636), *Malate dehydrogenase, cytoplasmic* (O88989), that form oxaloacetate, absence of *NADH dehydrogenase [ubiquinone] flavoprotein 2, mitochondrial* (P19234) that transfers electrons from NADH to respiratory chain in both groups treated with F, as well as the reduction of *ATP synthase subunit beta, mitochondrial* (P10719) (only in the group treated with the highest F dose), as well as the increase in *L-lactate dehydrogenase A chain* (P04642) in both groups treated with F indicate an increase in anaerobic metabolism in attempt to obtain energy, since aerobic metabolism is impaired in the presence of F. However, the rate of production of ATP through anaerobic pathways is much lower than that of aerobic pathways, which is in-line with the reports of reduction in the production of ATP induced by exposure to high F doses[3,54]. It is important to highlight that these changes in the expression of proteins associated to energy metabolism induced by exposure to 10 and 50 mgF/L in the drinking water are more pronounced than those observed previously in other organs exposed to roughly the same doses of F[9,10,30,55–58]. This might be due to the fact that the small intestine is responsible for the absorption of around 75% of ingested F[59], which makes the cells of the intestinal wall exposed to higher doses of F than the cells from the other organs.

In conclusion, chronic exposure to F, especially to the highest concentration evaluated, increased the thickness of the *tunica muscularis* and altered the pattern of protein expression. Extensive downregulation of several isoforms of histones might have contributed to the alterations found in the morphology of enteric neurons in response to F exposure. Additionally, changes in proteins involved in energy metabolism indicate a shift from aerobic to anaerobic metabolism upon exposure to the highest F concentration. These findings provide new insights into the mechanisms involved in F toxicity in the intestine.

References

1. Yan, X. *et al.* Fluoride induces apoptosis and alters collagen I expression in rat osteoblasts. *Toxicol Lett* **200**, 133–138, https://doi.org/10.1016/j.toxlet.2010.11.005 (2011).
2. Buzalaf, M. A., Pessan, J. P., Honorio, H. M. & ten Cate, J. M. Mechanisms of action of fluoride for caries control. *Monogr Oral Sci* **22**, 97–114, https://doi.org/10.1159/000325151 (2011).
3. Barbier, O., Arreola-Mendoza, L. & Del Razo, L. M. Molecular mechanisms of fluoride toxicity. *Chem Biol Interact* **188**, 319–333, https://doi.org/10.1016/j.cbi.2010.07.011 (2010).
4. Whitford, G. M. & Pashley, D. H. Fluoride absorption: the influence of gastric acidity. *Calcif Tissue Int* **36**, 302–307 (1984).
5. Nopakun, J., Messer, H. H. & Voller, V. Fluoride absorption from the gastrointestinal tract of rats. *J Nutr* **119**, 1411–1417 (1989).
6. Zheng, Y., Wu, J., Ng, J. C., Wang, G. & Lian, W. The absorption and excretion of fluoride and arsenic in humans. *Toxicol Lett* **133**, 77–82 (2002).
7. Susheela, A., Kumar, A., Bhatnagar, M. & Bahadur, R. Prevalence of endemic Fluorosis with gastrointestinal manifestations in People living in some North-Indian villages. *Fluoride* **26**, 97–104 (1993).
8. Susheela, A. *et al.* Fluoride ingestion and its correlation with gastrointestinal discomfort. *Fluoride* **25**, 5–22 (1992).
9. Sharma, J. D., Jain, P. & Sohu, D. Gastric Discomforts from Fluoride in Drinking Water in Sanganer Tehsil, Rajasthan, India. *Fluoride* **42**, 286–291 (2009).
10. Das, T. K., Susheela, A. K., Gupta, I. P., Dasarathy, S. & Tandon, R. K. Toxic Effects of Chronic Fluoride Ingestion on the Upper Gastrointestinal-Tract. *J Clin Gastroenterol* **18**, 194–199, https://doi.org/10.1097/00004836-199404000-00004 (1994).
11. Furness, J. B. A comprehensive overview of all aspects of the enteric nervous system. *The Enteric Nervous System*. (Blackwell, 2006).
12. Sand, E. *et al.* Structural and functional consequences of buserelin-induced enteric neuropathy in rat. *BMC Gastroenterol* **14**, 209, https://doi.org/10.1186/s12876-014-0209-7 (2014).
13. Melo, C. G. S. *et al.* Enteric innervation combined with proteomics for the evaluation of the effects of chronic fluoride exposure on the duodenum of rats. *Sci Rep* **7**, 1070, https://doi.org/10.1038/s41598-017-01090-y (2017).
14. Guyton, A. C. & Hall, J. E. *Textbook of medical physiology*. 13 edn, (Elsevier Health Sciences, 2015).
15. Dunipace, A. J. *et al.* Effect of aging on animal response to chronic fluoride exposure. *J Dent Res* **74**, 358–368, https://doi.org/10.1177/00220345950740011201 (1995).
16. Bradford, M. M. A rapid and sensitive method for the quantitation of microgram quantities of protein utilizing the principle of protein-dye binding. *Anal Biochem* **72**, 248–254 (1976).
17. Lima Leite, A. *et al.* Proteomic analysis of gastrocnemius muscle in rats with streptozotocin-induced diabetes and chronically exposed to fluoride. *PLoS One* **9**, e106646, https://doi.org/10.1371/journal.pone.0106646 (2014).
18. Bauer-Mehren, A. Integration of genomic information with biological networks using Cytoscape. *Methods Mol Biol* **1021**, 37–61, https://doi.org/10.1007/978-1-62703-450-0_3 (2013).
19. Millan, P. P. Visualization and analysis of biological networks. *Methods Mol Biol* **1021**, 63–88, https://doi.org/10.1007/978-1-62703-450-0_4 (2013).
20. Orchard, S. Molecular interaction databases. *Proteomics* **12**, 1656–1662, https://doi.org/10.1002/pmic.201100484 (2012).
21. Nopakun, J. & Messer, H. H. Mechanism of fluoride absorption from the rat small intestine. *Nutr Res* **10**, 771–779 (1990).
22. Vogt, R. L., Witherell, L., Lallue, D. & Klaucke, D. N. Acute fluoride poisoning associated with an on-site fluoridator in a Vermont elementary school. *Am J Public Health* **72**, 1168–1169 (1982).
23. Augenstein, W. L. *et al.* Fluoride ingestion in children: a review of 87 cases. *Pediatrics* **88**, 907–912 (1991).
24. Gessner, B. D., Beller, M., Middaugh, J. P. & Whitford, G. M. Acute fluoride poisoning from a public water system. *N Engl J Med* **330**, 95–99, https://doi.org/10.1056/NEJM199401133300203 (1994).
25. Akinbwa, K. Re-examination of acute toxicity of fluoride. *Fluoride* **30**, 89–104 (1997).
26. Holzer, P. & Lippe, I. T. Substance P can contract the longitudinal muscle of the guinea-pig small intestine by releasing intracellular calcium. *Brit J Pharmacol* **82**, 259–267 (1984).
27. Rivera, L. R., Poole, D. P., Thacker, M. & Furness, J. B. The involvement of nitric oxide synthase neurons in enteric neuropathies. *Neurogastroenterol Motil* **23**, 980–988, https://doi.org/10.1111/j.1365-2982.2011.01780.x (2011).
28. Benarroch, E. E. Enteric nervous system: functional organization and neurologic implications. *Neurology* **69**, 1953–1957, https://doi.org/10.1212/01.wnl.0000281999.56102.b6 (2007).

29. Defani, M. A., Zanoni, J. N., Natali, M. R., Bazotte, R. B. & de Miranda-Neto, M. H. Effect of acetyl-L-carnitine on VIP-ergic neurons in the jejunum submucous plexus of diabetic rats. *Arq Neuropsiquiatr* **61**, 962–967 (2003).
30. Ekelund, K. M. & Ekblad, E. Structural, neuronal, and functional adaptive changes in atrophic rat ileum. *Gut* **45**, 236–245 (1999).
31. Hermes-Uliana, C. *et al.* Is L-glutathione more effective than L-glutamine in preventing enteric diabetic neuropathy? *Dig Dis Sci* **59**, 937–948, https://doi.org/10.1007/s10620-013-2993-2 (2014).
32. Veli, A. P. & Zanoni, J. N. Age-related changes in myosin-V myenteric neurons, CGRP and VIP immunoreactivity in the ileum of rats supplemented with ascorbic acid. *Histol Histopathol* **27**, 123–132, https://doi.org/10.14670/HH-27.123 (2012).
33. Ekblad, E. & Bauer, A. J. Role of vasoactive intestinal peptide and inflammatory mediators in enteric neuronal plasticity. *Neurogastroenterol Motil* **16**(Suppl 1), 123–128, https://doi.org/10.1111/j.1743-3150.2004.00487.x (2004).
34. Ostz, M. *et al.* The intestinal trophic response to enteral food is reduced in parenterally fed preterm pigs and is associated with more nitrergic neurons. *J Nutr* **135**, 2657–2663 (2005).
35. Gabella, G. In *Physiology of the* Gastrointestinal Tract. (ed L. R. JOHNSON) 335–381 (Raven Press, 1987).
36. Soares, A., Beraldi, E. J., Ferreira, P. E., Bazotte, R. B. & Ballow, N. C. Intestinal and neuronal myenteric adaptations in the small intestine induced by a high-fat diet in mice. *BMC Gastroenterol* **15**, 3, https://doi.org/10.1186/s12876-015-0228-x (2015).
37. De Giorgio, R. *et al.* New insights into human enteric neuropathies. *Neurogastroenterol Motil* **16**(Suppl 1), 143–147, https://doi.org/10.1111/j.1743-3150.2004.00491.x (2004).
38. Gershon, M. D. & Ratcliffe, E. M. Developmental biology of the enteric nervous system: pathogenesis of Hirschsprung's disease and other congenital dysmotilities. *Semin Pediatr Surg* **13**, 224–235 (2004).
39. Bucci, C., Alifano, P. & Cogli, L. The role of rab proteins in neuronal cells and in the trafficking of neurotrophin receptors. *Membranes (Basel)* **4**, 642–677, https://doi.org/10.3390/membranes4040642 (2014).
40. Coune, P. G., Bensadoun, J. C., Aebischer, P. & Schneider, B. L. Rab1A over-expression prevents Golgi apparatus fragmentation and partially corrects motor deficits in an alpha-synuclein based rat model of Parkinson's disease. *J Parkinsons Dis* **1**, 373–387, https://doi.org/10.3233/JPD-2011-11058 (2011).
41. Lledo, P. M. *et al.* Rab3 proteins: key players in the control of exocytosis. *Trends Neurosci* **17**, 426–432 (1994).
42. Schlüter, O. M., Schmitz, F., Jahn, R., Rosenmund, C. & Südhof, T. C. A complete genetic analysis of neuronal Rab3 function. *J Neurosci* **24**, 6629–6637, https://doi.org/10.1523/JNEUROSCI.1610-04.2004 (2004).
43. Geppert, M., Goda, Y., Stevens, C. F. & Südhof, T. C. The small GTP-binding protein Rab3A regulates a late step in synaptic vesicle fusion. *Nature* **387**, 810–814, https://doi.org/10.1038/42954 (1997).
44. Li, J. Y., Jahn, R. & Dahlström, A. Rab3a, a small GTP-binding protein, undergoes fast anterograde transport but not retrograde transport in neurons. *Eur J Cell Biol* **67**, 297–307 (1995).
45. van Vlijmen, T. *et al.* A unique residue in rab3c determines the interaction with novel binding protein Zwint-1. *FEBS Lett* **582**, 2838–2842, https://doi.org/10.1016/j.febslet.2008.07.012 (2008).
46. Pavlos, N. J. *et al.* Rab3D regulates a novel vesicular trafficking pathway that is required for osteoclastic bone resorption. *Mol Cell Biol* **25**, 5253–5269, https://doi.org/10.1128/MCB.25.12.5253-5269.2005 (2005).
47. Valentijn, J. A., van Weeren, L., Ulfman, A. & Koster, A. J. Novel localization of Rab3D in rat intestinal goblet cells and Brunner's gland acinar cells suggests a role in early Golgi trafficking. *Am J Physiol Gastrointest Liver Physiol* **293**, G165–177, https://doi.org/10.1152/ajpgi.00520.2006 (2007).
48. Hoogenraad, C. C. *et al.* Neuron specific Rab4 effector GRASP-1 coordinates membrane specialization and maturation of recycling endosomes. *PLoS Biol* **8**, e1000283, https://doi.org/10.1371/journal.pbio.1000283 (2010).
49. de Hoop, M. J. *et al.* The involvement of the small GTP-binding protein Rab5a in neuronal endocytosis. *Neuron* **13**, 11–22 (1994).
50. Gerges, N. Z., Backos, D. S. & Esteban, J. A. Local control of AMPA receptor trafficking at the postsynaptic terminal by a small GTPase of the Rab family. *J Biol Chem* **279**, 43870–43878, https://doi.org/10.1074/jbc.M404982200 (2004).
51. Saifdharan, N. *et al.* RAB-5 and RAB-10 cooperate to regulate neuropeptide release in Caenorhabditis elegans. *Proc Natl Acad Sci USA* **109**, 18944–18949, https://doi.org/10.1073/pnas.1203306109 (2012).
52. Zou, W., Yadav, S., DeVault, L., Nung Jan, Y. & Sherwood, D. R. RAB-10-Dependent Membrane Transport Is Required for Dendrite Arborization. *PLoS Genet* **11**, e1005484, https://doi.org/10.1371/journal.pgen.1005484 (2015).
53. Strohl, K. *et al.* M98K-OPTN induces transferrin receptor degradation and RAB12-mediated autophagic death in retinal ganglion cells. *Autophagy* **9**, 510–527, https://doi.org/10.4161/auto.23458 (2013).
54. Binotti, B. *et al.* The GTPase Rab26 links synaptic vesicles to the autophagy pathway. *Elife* **4**, e05597, https://doi.org/10.7554/eLife.05597 (2015).
55. Villarroel-Campos, D. *et al.* Rab35 Functions in Axon Elongation Are Regulated by P53-Related Protein Kinase in a Mechanism That Involves Rab35 Protein Degradation and the Microtubule-Associated Protein 1B. *J Neurosci* **36**, 7298–7313, https://doi.org/10.1523/JNEUROSCI.4064-15.2016 (2016).
56. Sano, H. *et al.* Rab10, a target of the AS160 Rab GAP, is required for insulin-stimulated translocation of GLUT4 to the adipocyte plasma membrane. *Cell metabolism* **5**, 293–303, https://doi.org/10.1016/j.cmet.2007.03.001 (2007).
57. Brewer, P. D., Habtemichael, E. N., Romenskaia, I., Coster, A. C. & Mastick, C. C. Rab14 limits the sorting of Glut4 from endosomes into insulin-sensitive regulated secretory compartments in adipocytes. *The Biochemical J* **473**, 1315–1327, https://doi.org/10.1042/BCJ20160020 (2016).
58. Lobo, J. G. *et al.* Low-Level Fluoride Exposure Increases Insulin Sensitivity in Experimental Diabetes. *J Dent Res* **94**, 990–997, https://doi.org/10.1177/0022034515581186 (2015).
59. Lang, J. Molecular mechanisms and regulation of insulin exocytosis as a paradigm of endocrine secretion. *Eur J Biochem* **259**, 3–17 (1999).
60. Ljubicic, S. *et al.* The GTPase Rab37 Participates in the Control of Insulin Exocytosis. *PLoS One* **8**, e68255, https://doi.org/10.1371/journal.pone.0068255 (2013).
61. Lehninger, A. L., Nelson, D. L. & Cox, M. M. *Lehninger principles of biochemistry*. 3. ed. edn, 975 (2002).
62. Xiong, X. *et al.* Dose-effect relationship between drinking water fluoride levels and damage to liver and kidney functions in children. *Environ Res* **103**, 112–116, https://doi.org/10.1016/j.envres.2006.05.008 (2007).
63. Ge, Y., Niu, R., Zhang, J. & Wang, J. Proteomic analysis of brain proteins of rats exposed to high fluoride and low iodine. *Arch Toxicol* **85**, 27–33, https://doi.org/10.1007/s00204-010-0537-5 (2011).
64. Kaminsky, L. S. & Zhang, Q. Y. The small intestine as a xenobiotic-metabolizing organ. *Drug Metab Dispos* **31**, 1520–1525, https://doi.org/10.1124/dmd.31.12.1520 (2003).
65. Ciechanover, A. & Schwartz, A. L. The ubiquitin-proteasome pathway: the complexity and myriad functions of proteins death. *Proc Natl Acad Sci USA* **95**, 2727–2730 (1998).
66. Bottermann, K., Reinartz, M., Barsoum, M., Kotter, S. & Godecke, A. Systematic Analysis Reveals Elongation Factor 2 and alpha-Enolase as Novel Interaction Partners of AKT2. *PLoS One* **8**, e66045, https://doi.org/10.1371/journal.pone.0066045 (2013).
67. Norrander, J., Larsson, M., Stähl, S., Höög, C. & Linck, R. Expression of ciliary tektins in brain and sensory development. *J Neurosci* **18**, 8912–8918 (1998).
68. Waterhouse, N. J. *et al.* Cytotoxic T lymphocyte-induced killing in the absence of granzymes A and B is unique and distinct from both apoptosis and perforin-dependent lysis. *J Cell Biol* **173**, 133–144, https://doi.org/10.1083/jcb.200510072 (2006).
69. Pipkin, M. E. & Lieberman, J. Delivering the kiss of death: progress on understanding how perforin works. *Curr Opin Immunol* **19**, 301–308, https://doi.org/10.1016/j.coi.2007.04.011 (2007).

70. Meuth, S. G. et al. Cytotoxic CD8+ T cell–neuron interactions: perforin-dependent electrical silencing precedes but is not causally linked to neuronal cell death. *J Neurosci* **29**, 15397–15409, https://doi.org/10.1523/JNEUROSCI.4339-09.2009 (2009).
71. Perfettini, J. L., Roumier, T. & Kroemer, G. Mitochondrial fusion and fission in the control of apoptosis. *Trends Cell Biol* **15**, 179–183, https://doi.org/10.1016/j.tcb.2005.02.005 (2005).
72. Chen, H. & Chan, D. C. Emerging functions of mammalian mitochondrial fusion and fission. *Hum Mol Genet 14 Spec No. 2*, R283–289, https://doi.org/10.1093/hmg/ddi270 (2005).
73. James, D. I., Parone, P. A., Mattenberger, Y. & Martinou, J. C. hFis1, a novel component of the mammalian mitochondrial fission machinery. *J Biol Chem* **278**, 36373–36379, https://doi.org/10.1074/jbc.M303758200 (2003).
74. Gomes, L. C. & Scorrano, L. High levels of Fis1, a pro-fission mitochondrial protein, trigger autophagy. *Biochim Biophys Acta* **1777**, 860–866, https://doi.org/10.1016/j.bbabio.2008.05.442 (2008).
75. Wang, Y. et al. Neuroprotective Effect and Mechanism of Thiazolidinedione on Dopaminergic Neurons *In Vivo* and *In Vitro* in Parkinson's Disease. *PPAR Res* **2017**, 4089214, https://doi.org/10.1155/2017/4089214 (2017).
76. Hofmann, B., Hecht, H. J. & Flohe, L. Peroxiredoxins. *Biol Chem* **383**, 347–364, https://doi.org/10.1515/BC.2002.040 (2002).
77. Shanthakumari, D., Srinivasalu, S. & Subramanian, S. Effect of fluoride intoxication on lipidperoxidation and antioxidant status in experimental rats. *Toxicology* **204**, 219–228, https://doi.org/10.1016/j.tox.2004.06.058 (2004).
78. Stirnimann, G., Kessebohm, K. & Lauterburg, B. Liver injury caused by drugs: an update. *Swiss Med Wkly* **140**, w13080, https://doi.org/10.4414/smw.2010.13080 (2010).
79. Zhan, X. A., Wang, M., Xu, Z. R., Li, W. F. & Li, J. X. Effects of fluoride on hepatic antioxidant system and transcription of Cu/Zn SOD gene in young pigs. *J Trace Elem Med Biol* **20**, 83–87, https://doi.org/10.1016/j.jtemb.2005.11.003 (2006).
80. Pereira, H. A. et al. Proteomic analysis of liver in rats chronically exposed to fluoride. *PLoS One* **8**, e75343, https://doi.org/10.1371/journal.pone.0075343 (2013).
81. Pereira, H. A. et al. Fluoride Intensifies Hypercaloric Diet-Induced ER Oxidative Stress and Alters Lipid Metabolism. *PLoS One* **11**, e0158121, https://doi.org/10.1371/journal.pone.0158121 (2016).
82. Maze, I., Noh, K. M., Soshnev, A. A. & Allis, C. D. Every amino acid matters: essential contributions of histone variants to mammalian development and disease. *Nat Rev Genet* **15**, 259–271, https://doi.org/10.1038/nrg3673 (2014).
83. Riccio, A. Dynamic epigenetic regulation in neurons: enzymes, stimuli and signaling pathways. *Nat Neurosci* **13**, 1330–1337, https://doi.org/10.1038/nn.2671 (2010).
84. Strunecka, A., Patocka, J., Blaylock, R. & Chinoy, N. Fluoride interactions: from molecules to disease. *Current Signal Transduction Therapy* **2**, 190–213 (2007).
85. Xu, H. et al. Proteomic analysis of kidney in fluoride-treated rat. *Toxicol Lett* **160**, 69–75, https://doi.org/10.1016/j.toxlet.2005.06.009 (2005).
86. Kobayashi, C. A. et al. Proteomic analysis of kidney in rats chronically exposed to fluoride. *Chem Biol Interact* **180**, 305–311, https://doi.org/10.1016/j.cbi.2009.03.009 (2009).
87. Niu, R. *et al.* Proteomic analysis of hippocampus in offspring male mice exposed to fluoride and lead. *Biol Trace Elem Res* **162**, 227–233, https://doi.org/10.1007/s12011-014-0117-2 (2014).
88. Carvalho, J. G. et al. Renal proteome in mice with different susceptibilities to fluorosis. *PLoS One* **8**, e53261, https://doi.org/10.1371/journal.pone.0053261 (2013).
89. Bindea, G., Galon, J. & Mlecnik, B. CluePedia Cytoscape plugin: pathway insights using integrated experimental and in silico data. *Bioinformatics* **29**, 661–663, https://doi.org/10.1093/bioinformatics/btt019 (2013).
90. Bindea, G. et al. ClueGO: a Cytoscape plug-in to decipher functionally grouped gene ontology and pathway annotation networks. *Bioinformatics* **25**, 1091–1093, https://doi.org/10.1093/bioinformatics/btp101 (2009).

Acknowledgements

This study was supported by FAPESP (2011/10233-7, 2012/16840-5 and 2016/09100-6).

Author Contributions

C.M., M.B., J.Z., and J.P. conceived the experiments. A.D., C.M., J.P., S.S. and A.L. conducted the experiments. A.D., C.M., J.P., S.S., A.L., I.A., T.V., A.H., and J.S. participated in the research experiments. A.D., C. M., A.H., J.S., E.S. participated in the experiments analysis. A.D., C.M., M.B. drafted the article; analyzed and interpreted the results. All authors reviewed and approved the manuscript.

Additional Information

Supplementary information accompanies this paper at https://doi.org/10.1038/s41598-018-21533-4.

Competing Interests: The authors declare no competing interests.

Publisher's note: Springer Nature remains neutral with regard to jurisdictional claims in published maps and institutional affiliations.

ANEXO D – **ARTIGO PUBLICADO SCIENCE OF THE TOTAL ENVIRONMENT (ARTIGO 3)**

Science of the Total Environment 741 (2020) 140419

Contents lists available at ScienceDirect

Science of the Total Environment

journal homepage: www.elsevier.com/locate/scitotenv

Effects of acute fluoride exposure on the jejunum and ileum of rats: Insights from proteomic and enteric innervation analysis

Aline Dionizio [a], Carina Guimarães Souza Melo [a], Isabela Tomazini Sabino-Arias [a], Tamara Teodoro Araujo [a], Talita Mendes Oliveira Ventura [a], Aline Lima Leite [a], Sara Raquel Garcia Souza [b], Erika Xavier Santos [b], Alessandro Domingues Heubel [a], Juliana Gadelha Souza [a], Juliana Vanessa Colombo Martins Perles [b], Jacqueline Nelisis Zanoni [b], Marília Afonso Rabelo Buzalaf [a,*]

[a] Department of Biological Sciences, Bauru School of Dentistry, University of São Paulo, Bauru, Brazil
[b] Department of Morphophysiological Sciences, State University of Maringá, Maringá, Brazil

HIGHLIGHTS

- Water containing 25 mgF/Kg bw F provokes morphological changes and alters in several proteins in the jejunum and ileum;
- Organism might not have had time to adapt to its toxic effect. Therefore, the loss of energy may have not been repaired.
- Morphological changes in the gut, can be explained by alterations in VIP-IR and in proteins that regulate the cytoskeleton.

GRAPHICAL ABSTRACT

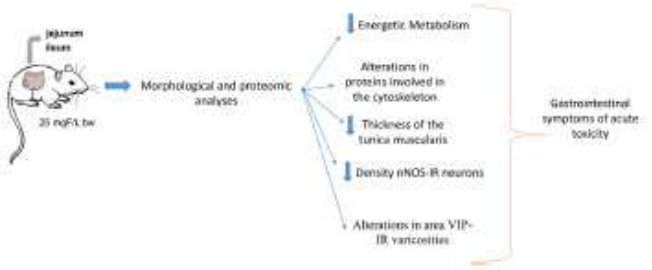

ARTICLE INFO

Article history:
Received 27 March 2020
Received in revised form 4 June 2020
Accepted 20 June 2020
Available online 22 June 2020

Editor: Lotfi Aleya

Keywords:
Fluoride
Acute
Chronic
Ileum
Jejunum

ABSTRACT

Fluoride (F) is largely employed in dentistry, in therapeutic doses, to control caries. However, excessive intake may lead to adverse effects in the body. Since F is absorbed mostly from the gastrointestinal tract (GIT), gastrointestinal symptoms are the first signs following acute F exposure. Nevertheless, little is known about the mechanistic events that lead to these symptoms. Therefore, the present study evaluated changes in the proteomic profile as well as morphological changes in the jejunum and ileum of rats upon acute exposure to F. Male rats received, by gastric gavage, a single dose of F containing 0 (control) or 25 mg/Kg for 30 days. Upon exposure to F, there was a decrease in the thickness of the tunic muscularis for both segments and a decrease in the thickness of the wall only for the ileum. In addition, a decrease in the density of HuC/D-IR neurons and nNOS-IR neurons was found for the jejunum, but for the ileum only nNOS-IR neurons were decreased upon F exposure. Moreover, SP-IR varicosities were increased in both segments, while VIP-IR varicosities were increased in the jejunum and decreased in the ileum. As for the proteomic analysis, the proteins with altered expression were mostly negatively regulated and associated mainly with protein synthesis and energy metabolism. Proteomics also revealed alterations in proteins involved in oxidative/antioxidant defense, apoptosis and as well as in cytoskeletal proteins. Our results, when analyzed together, suggest that the gastrointestinal symptoms found in cases of acute F exposure might be related to the morphological alterations in the gut (decrease in the thickness of the tunica muscularis)

Abbreviations: HuC/D-IR, immunoreactive to human proteins type C and D; nNOS-IR, immunoreactive to neural nitric oxide synthase; SP-IR, immunoreactive to substance P; VIP-IR, immunoreactive to intestinal vasoactive peptide; CGRP-IR, immunoreactive to calcitonin gene-related peptide.

* Corresponding author at: Alameda Octávio Pinheiro Brisolla, 9-75, Bauru, SP 17012-901, Brazil.
E-mail address: mburalaf@fob.usp.br (M.A.R. Buzalaf).

https://doi.org/10.1016/j.scitotenv.2020.140419
0048-9697/

that, at the molecular level, can be explained by alterations in the gut vipergic innervation and in proteins that regulate the cytoskeleton.

1. Introduction

Fluorine is one of the most abundant elements in the earth's crust (Shanthakumari et al., 2004) and is found in its ionic form (fluoride; F) in biological fluids and tissues as a trace element, in two different forms: inorganic and organic, being 99% accumulated in hard tissues (Suarez et al., 2008). F is widely used as a therapeutic agent against caries and can be found naturally in soil and water or in controlled doses at water supply stations (McDonagh et al., 2000; Wong et al., 2011). However, studies have shown that excessive intake of F can lead to side effects (Buzalaf et al., 2013; Whitford, 1996; Yan et al., 2011) perceived at the molecular level (Araujo et al., 2019; Barbier et al., 2010), as well as at the tissue level in several organs and structures, such as skeletal muscles, brain, spinal column (Mullenix et al., 1995), liver (Dionizio et al., 2019; Pereira et al., 2018; Pereira et al., 2016; Pereira et al., 2013) and gut (Dionizio et al., 2018; Melo et al., 2017).

The toxic effect of F is related to the amount and duration of exposure (Araujo et al., 2019; Dionizio et al., 2019; Pereira et al., 2018) and can be classified into acute or chronic (He and Chen, 2006; Shanthakumari et al., 2004; Whitford, 1992). Acute toxicity occurs by ingesting a large amount of F at a single time (Whitford, 2011). Most of the studies evaluating acute F exposure report the effects at the molecular and histological levels in the kidney (Jimenez-Cordova et al., 2019; Mitsui et al., 2010; Santoyo-Sanchez et al., 2013) and heart (Mitsui et al., 2007; Panneerselvam et al., 2019). Considering that the gastrointestinal tract (GIT), especially the gut, is the main responsible for the absorption of F (Nopakun et al., 1989; Whitford, 2011; Whitford and Pashley, 1984), gastrointestinal manifestations are frequently reported in cases of acute F intoxication, such as vomiting with blood and diarrhea. These manifestations can occur in cases of professional application of F for caries prevention, especially in children, as well as in cases of poisoning (Whitford, 2011). However, little is known regarding the effects of acute F exposure in the GIT at the molecular level. This knowledge is important to allow an adequate treatment of patients submitted to acute F intoxication. In this sense, the present study attempted to shed light into the molecular mechanisms underlying acute F toxicity, by performing morphological analysis of the intestinal wall and myenteric neurons, as well as proteomic analysis of the jejunum and ileum of rats, after acute exposure to F.

2. Material and methods

2.1. Animals and treatment

The work was performed on twelve adult male rats (60 days of life – *Rattus norvegicus*, Wistar type). The animals were individually housed in metabolic cages, with *ad libitum* access to deionized water and low-fluoride chow for 30 days. The illumination (12 h light/12 dark hours) and the ambient temperature were controlled (22 ± 2 °C). The animals were randomly divided into 2 groups ($n = 6$ per group), according with the treatment they received by gavage in the last day of the experiment. The experimental group received 25 mgF/kg body weight as sodium fluoride (NaF) dissolved in deionized water, while the control group received deionized water. As rodents metabolize F 5 times faster than humans (Dunipace et al., 1995), this dose of F corresponds to ~5 mg/kg to humans, which corresponds to the probable toxic dose (PTD) (Whitford, 2011). After the treatment period, the plasma was obtained by centrifugation of blood at 800*g* for 5 min for quantification of F, as previously described (Melo et al., 2017). Then, the jejunum and ileum were collected as described by Dionizio et al. (2018), for morphological and proteomic analysis. Briefly, animal chow was removed from the animals 18 h prior to euthanasia, to reduce the volume of fecal material inside the small intestine, thus making easier the cleaning process for posterior analysis. After identifying the duodenojejunal flexure, one incision is made. Around 20 cm were despised and then 15 cm of the jejunum were harvested. After localizing the cecum, two incisions were made to collect the ileum: one in the anterior portion of the ileocecal valve and the other 10 cm proximally to the first one. The jejunum and ileum segments were washed with phosphate buffered solution several times to remove residues of fecal material. All experimental protocols were approved by the Animal Experimentation Ethics Committee of the Faculty of Dentistry of Bauru of the University of São Paulo (protocols 014/2011 and 012/2016).

2.2. Histological analysis and myenteric plexus immunohistochemistry, morphometric and semi-quantitative analysis

These analyses were performed exactly as described by Melo et al. (2017)

2.3. Proteomics and bioinformatics analyses

The frozen jejunum and ileum were homogenized in a cryogenic mill (model 6770, Spex, Metuchen, NJ, EUA). Samples from 2 animals were pooled and analyses were carried out in triplicates, exactly as previously described (Dionizio et al., 2018). Briefly, protein extraction was performed by incubation in lysis buffer (7 M urea, 2 M thiourea, 40 mM DTT, all diluted in AMBIC solution) under constant stirring at 4 °C. After centrifugation at 20,817*g* for 30 min at 4 °C, the supernatant was collected and total protein was quantified (Bradford, 1976). To 50 μL of each sample (containing 50 μg protein) 25 μL of 0.2% Rapigest (Waters cat#186001861) were added, followed by agitation and then 10 μL 50 mM AMBIC were added, followed by incubation for 30 min at 37 °C. Samples were then reduced (100 mM DTT; BioRad, cat# 161-0611) and alkylated (300 mM IAA; GE, cat# RPN 6302 V) under dark at room temperature for 30 min. Digestion was performed at 37 °C overnight by adding 100 ng trypsin (Promega, cat#V5280). Then 10 μL of 5% TFA were added, samples were incubated for 90 min at 37 °C and centrifuged (20,817 *g* at 6 °C for 30 min). Supernatant was purified using C 18 Spin columns (Pierce, cat #89870). Samples were then resuspended in 200 μL 3% acetonitrile.

The peptides identification was performed on a nanoAcquity UPLC-Xevo QTof MS system (Waters, Manchester, UK), as previously described (Lima Leite et al., 2014). The Protein Lynx Global Server (PLGS) software was used to detect difference in expression between the groups, which was expressed as $p < 0.05$ and $1\text{-}p > 0.95$ for down- and up-regulated proteins, respectively. Bioinformatics analysis was performed for comparison of the treated group with the control group (Tables S1–S2), as earlier reported (Bauer-Mehren, 2013; Lima Leite et al., 2014; Millan, 2013; Orchard, 2012). The software CYTOSCAPE® 3.0.4 (Java®) was employed to build networks of molecular interaction between the identified proteins, with the support of ClusterMarker® application.

3. Results

3.1. Morphological analysis of the jejunum and ileum wall thickness

The mean (±SD) thickness of the tunica muscularis was significantly decreased in the treated groups of jejunum (90.1 ± 1.9 μm²) and ileum (134.0 ± 2.5 μm²) when compared with the respective controls (116.4 ± 3.7 μm² and 223.6 ± 7.8 μm²) (Student's t-test, $p < 0.05$). The same was observed for the mean (±SD) total thickness of the wall, which was significantly reduced in the treated group (756.5 ± 12.9 μm²) when compared with control (784.1 ± 17.1 μm²) for ileum (Student's t-test, $p > 0.05$).

3.2. Myenteric neurons HuC/D – IR analysis

In the morphometric analysis of the general population of neurons, after treatment with fluoride, the cell bodies areas of the HuC/D–IR neurons of the ileum (μm²) were significantly increased, but no significant changes were seen in the jejunum ($p > 0.05$). In the quantitative analyses, the treated group presented a significant decrease in the jejunum but was not significantly altered in the ileum ($p > 0.05$). (Tables 1 and 2).

3.3. Myenteric neurons nNOS –IR analysis

In the morphometric analysis of the general population of neurons, the cell bodies areas of the nNOS–IR neurons (μm²) were significantly increased in the jejunum and significantly decreased in the ileum, in comparison with the respective controls ($p < 0.05$). In the quantitative analyses, significant decreases were observed in the treated groups in respect to control, both for jejunum and ileum ($p < 0.05$) (Tables 1 and 2).

3.4. Myenteric neurons VIP-IR, CGRP-IR and SP-IR morphometric analysis

In the morphometric analyses of the SP-IP varicosities (μm²) a significant increase was detected in the treated groups in respect to control, both for jejunum and ileum ($p < 0.05$). CGRP–IR varicosities (μm²) were significantly reduced in the ileum after treatment with fluoride but were not significantly altered in the jejunum ($p > 0.05$). The VIP–IR varicosities (μm²) were significantly increased in the jejunum and significantly decreased in the ileum upon treatment with fluoride ($p < 0.05$) (Tables 1 and 2). Representative images of the immunofluorescences are displayed in supplementary information (Supplementary Figs. S1–S4).

Table 1
Means and standard errors of the values of the cell bodies areas and density of HUC/D-IR, nNOS-IR and VIP-IR, CGRP-IR, and SP-IR values of myenteric neurons varicosities areas of the **jejunum** of rats exposed or not to acute dose of F. Animal groups: Control (deionized water - 0 mgF/L) and 25mgF/Kg bw.

Analysis	Control	25mgF/Kg bw
Cell bodies areas of the HuC/D-IR neurons (μm²)	319.5 ± 3.5[a]	316.2 ± 3.9[a]
Density HuC/D-IR neurons (neurons/cm²)	16,584.0 ± 343.1[a]	13,848.4 ± 324.3[b]
Cell bodies areas of the nNOS-IR neurons (μm²)	288.7 ± 3.0[a]	300.8 ± 3.0[b]
Density nNOS-IR neurons (neurons/cm²)	5959.9 ± 138.7[a]	5219.9 ± 151.6[b]
Area VIP-IR varicosities (μm²)	2.8 ± 0.0[a]	3.0 ± 0.0[b]
Area CGRP-IR varicosities (μm²)	3.5 ± 0.0[a]	3.5 ± 0.0[a]
Area SP-IR varicosities (μm²)	3.1 ± 0.0[a]	4.8 ± 0.0[b]

Means followed by different letters in the same column are significantly different according to Student's t-test ($p < 0.05$). (N = 6).

Table 2
Means and standard errors of the values of the cell bodies areas and density of HUC/D-IR, nNOS-IR and VIP-IR, CGRP-IR, and SP-IR values of myenteric neurons varicosities areas of the **ileum** of rats exposed or not to acute dose of F. Animal groups: Control (deionized water - 0 mgF/L) and 25mgF/Kg bw.

Analysis	Control	25mgF/Kg bw
Cell bodies areas of the HuC/D-IR neurons (μm²)	298.0 ± 3.6[a]	312.3 ± 4.0[b]
Density HuC/D-IR neurons (neurons/cm²)	13,099.8 ± 420.9[a]	12,756.9 ± 347.7[a]
Cell bodies areas of the nNOS-IR neurons (μm²)	300.4 ± 3.3[a]	287.6 ± 3.1[b]
Density nNOS-IR neurons (neurons/cm²)	4657.1 ± 145.4[a]	3905.6 ± 129.7[b]
Area VIP-IR varicosities (μm²)	3.3 ± 0.0[a]	3.1 ± 0.0[b]
Area CGRP-IR varicosities (μm²)	3.4 ± 0.0[a]	3.2 ± 0.0[b]
Area SP-IR varicosities (μm²)	2.9 ± 0.0[a]	4515 ± 0.0[b]

Means followed by different letters in the same line are significantly different according to Student's t-test ($p < 0.05$). (N = 6).

3.5. Proteomic analysis

The total numbers of proteins identified by mass spectrometry in jejunum of control and treated group were 282 and 227, respectively. Among them, 106 and 51 proteins were uniquely identified in the control and treated groups, respectively. In the quantitative analysis of treated *vs.* control group, 37 proteins with change in expression were detected. Most of the proteins with altered expression were downregulated in the group treated with F when compared with the control group (23 proteins), suggesting that acute exposure to F reduces protein synthesis (Table S1).

Fig. 1 shows the subnetworks generated by ClusterMarker® for the comparison treated *vs.* control group of jejunum. Most of the proteins with altered expression interacted with *Dynein light chain 1, cytoplasmic (P63170)*, *Solute carrier family 2, facilitated glucose transporter member 4 (P19357)*, *Polyubiquitin-C (Q63429)*, *Gap junction alpha-1 protein (P08050)*, *Protein deglycase DJ-1 (O88767)*, *Small ubiquitin-related modifier 3 (Q5XIF4)* (Fig. 1A) or *Heterogeneous nuclear ribonucleoprotein K (P61980)* and *Mitogen-activated protein kinase 3 (P21708)* (Fig. 1B).

Fig. 2 shows the functional classification according to the biological process with the most significant term, for the comparison between treated *vs.* control group for jejunum. Among them, the categories with the highest percentages of genes were Actin filament binding (14.1%), Calmodulin binding (14.1%), Structural constituent of cytoskeleton (12.5%), Motor activity (10.9%) and Hydrogen ion transmembrane transporter activity (9.4%).

The total numbers of proteins identified by mass spectrometry in the ileum for control and treated groups were 195 and 183, respectively. Among them, 66 and 54 proteins were uniquely identified in the control and treated groups, respectively. In the quantitative analysis of the treated *vs.* control group, 36 proteins with change in expression were detected. Most of the proteins with altered expression were downregulated in the group treated with F when compared with the control group (22 proteins), suggesting that acute exposure to F reduces protein synthesis (Table S2).

Fig. 3 shows the subnetworks generated by ClusterMarker® for the treated *vs.* control group of ileum. Most of the proteins with altered expression interacted with *Solute carrier family 2, facilitated glucose transporter member 4* (P19357), *Heterogeneous nuclear ribonucleoprotein K* (P61980), *UV excision repair protein RAD23 homolog B* (Q4KMA2), *Protein deglycase DJ-1* (O88767) and *Polyubiquitin-C* (Q63429) (Fig. 3A) or *Mitogen-activated protein kinase 3* (P21708) and *Gap junction alpha-1 protein* (P08050) (Fig. 3B).

Fig. 4 shows the functional classification according to the biological process with the most significant term, for the comparison between treated *vs.* control groups for ileum. Among them, the categories with the highest percentages of genes were Intermediate filament-based

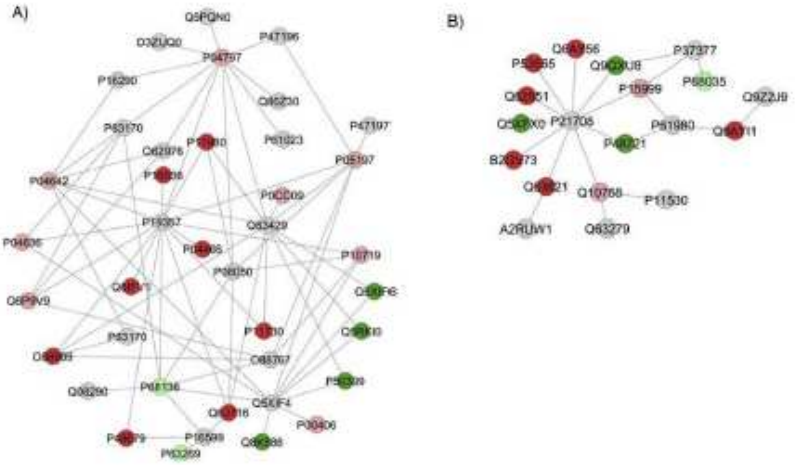

Fig. 1. Subnetworks created by ClusterMarker® to establish the interaction between proteins identified with differential expression in the 25 mgF/Kg wb group in relation to the control group in jejunum. The color of the nodes indicates the differential expression of the respective named protein with its access code. The dark red and dark green nodes indicate proteins unique to the control and 25 mgF/Kg wb groups, respectively. The nodes in gray indicate the interaction proteins that are offered by CYTOSCAPE®, which were not identified in the present study and the light red and light green nodes indicate downregulation and upregulation, respectively. In A the access numbers in the gray nodes correspond to: *RAC-beta serine/threonine-protein kinase (P47197), RAC-alpha serine/threonine-protein kinase (P47196), Neurocalcin-delta (Q5RJN0), RILP-like protein 1 (D3ZUQ0), Phosphoglycerate mutase 2 (P16290), Dynein light chain 1, cytoplasmic (P63170), Calcium-activated potassium channel subunit alpha-1 (Q62976), Protein phosphatase 1E (Q80Z80), Calcineurin B homologous protein 1 (P63023), Solute carrier family 2, facilitated glucose transporter member 4 (P19357), Polyubiquitin-C (Q63429), Gap junction alpha-1 protein (P08050), Dynein light chain 1, cytoplasmic (P63170), Protein deglycase DJ-1 (O88767), Small ubiquitin-related modifier 3 (Q5XIF4), Tumor necrosis factor* (P16599) and *Calpain-1* (Q08290). The access numbers of the unique proteins of the control (dark red nodes) correspond to the: *Pyruvate kinase PKM* (P11980), *Phosphate carrier protein, mitochondrial* (P16036), *Myosin regulatory light chain 2, skeletal muscle isoform* (P04466), *Keratin, type I cytoskeletal 14* (Q6IFV1), *Calcium/calmodulin-dependent protein kinase type II subunit gamma* (P11730), *Malate dehydrogenase, cytoplasmic* (O88989), *Peroxiredoxin-1* (Q63716) and *Prelamin-A/C* (P48679). The accession numbers of the unique 25 mgF/Kg wb (dark green nodes) proteins correspond to the: *Tubulin alpha-4A chain* (Q5XIF6), *WD repeat-containing protein 1* (Q5RKI0), *Rab GDP dissociation inhibitor beta* (P50399) and *GTP-binding nuclear protein Ran, testis-specific isoform* (Q8K586). The access numbers of the downregulated proteins (light red nodes) correspond to the: *Glyceraldehyde-3-phosphate dehydrogenase* (P04797), *L-lactate dehydrogenase A chain* (P04642), *Elongation factor 2* (P05197), *Histone H2A type 2-A* (P0CC09), *Malate dehydrogenase, mitochondrial* (P04636), *Tubulin alpha-1B chain* (Q6P9V9), *ATP synthase subunit beta, mitochondrial* (P10719) and *Cytochrome c oxidase subunit 2* (P00406). The access numbers of the upregulated proteins (light green nodes) correspond to the: *Actin, gamma-enteric smooth muscle* (P63269) and *Actin, alpha skeletal muscle* (P68136). In B the access numbers in the gray nodes correspond to: *Alpha-synuclein* (P37377), *Runt-related transcription factor 2* (Q9ZJ9), *Heterogeneous nuclear ribonucleoprotein K* (P61980), *Mitogen-activated protein kinase 3* (P21708), *Dystrophin* (P11530), *Keratin, type I cytoskeletal 19* (Q63279) and *Toll-interacting protein* (A2RUW1). The access numbers of the unique proteins of the control (dark red nodes) correspond to the: *Tubulin alpha-8 chain* (Q6AYS6), *Homeobox protein cut-like 1* (P53565), *Delta(3,5)-Delta (2,4)-dienoyl-CoA isomerase, mitochondrial* (Q62651), *Actin-related protein 2/3 complex subunit 3* (B2GV73), *Interleukin-1 receptor accessory protein* (Q63621) and *DEAD (Asp-Glu-Ala-Asp) box polypeptide 5* (Q6AYI1). The accession numbers of the unique 25 mgF/Kg wb (dark green nodes) proteins correspond to the: *Cytoplasmic dynein 1 light intermediate chain 1* (Q9QXJ8), *Triangulin-2* (Q5XFX0) and *Stress-70 protein, mitochondrial* (P48721). The access numbers of the downregulated proteins (light red nodes) correspond to the: *ATP synthase subunit alpha, mitochondrial* (P15999) and *Keratin, type II cytoskeletal 8* (Q10758). The access numbers of the upregulated proteins (light green nodes) correspond to the à: *Actin, alpha cardiac muscle 1* (P68035). (For interpretation of the references to color in this figure legend, the reader is referred to the web version of this article.)

process (21%), Oxygen transport (12%), Regulation of mitochondrial membrane permeability involved in apoptotic process (9%), Positive regulation of lipid kinase activity (9%) and Cellular response to nitric oxide (6%).

4. Discussion

The present study was designed to evaluate proteomic and morphological alterations in the jejunum after acute exposure to F. The dose we administered to rats (25 mgF/kg body weight) mimics the probable toxic dose (PTD) for humans, which is 5 mgF/Kg body weight (Whitford, 2011). This happens because rodents metabolize F 5 times faster than humans (Dunipace et al., 1995). We did not attempt to simulate the therapeutic doses of F for caries control, since in this case we usually have lower doses of fluoride administered along time, *i.e.*, chronic exposure, which was evaluated in our previous studies (Dionizio et al., 2018; Melo et al., 2017). However, in cases of topical F application of fluoridated gels, especially in younger children, the PTD related to acute exposure can be reached and gastrointestinal signals and symptoms might be observed (Whitford, 2011).

Under acute exposure to F, the majority of the proteins with altered expression were downregulated, both in jejunum (Table S1) and ileum (Table S2). These results indicate that acute exposure to F reduced protein synthesis in distinct segments of the gut. The *subnetworks* for the comparison between the group treated with 25 mgF/Kg bw vs. control, both for jejunum (Fig. 1) and ileum (Fig. 3), revealed that most of the proteins with altered expression interacted with *Solute carrier family 2 facilitated glucose transporter member 4* (GLUT4; P19357), *Polyubiquitin-C* (Q63429), *Mitogen-activated protein kinase 3* (MAPK3; P21708) or *Heterogeneous nuclear ribonucleoprotein K* (P61980). Interestingly, the first 3 interacting partners were also present in the *subnetwork* comparing the proteins differentially expressed in the jejunum of rats chronically treated with 50 mgF/L F when compared with control (Dionizio et al., 2018). GLUT4 is involved in glucose transport. In a recent report by our group, in which proteomic analysis was conducted in the muscle and liver of diabetic rats, we observed that exposure to F altered many proteins that interacted with GLUT4 and could impair its function (Lima Leite et al., 2014; Lobo et al., 2015). In the present study, a plethora of proteins that interacted with GLUT4 and are involved in energy metabolism, especially of carbohydrates, were reduced or even absent in the jejunum upon acute exposure to F, such as *Malate dehydrogenase, mitochondrial* (P04636), *Malate dehydrogenase, cytoplasmic* (O88989), *L-lactate dehydrogenase A chain* (P04642), *Pyruvate kinase PKM* (P11980) and *Glyceraldehyde-3-phosphate dehydrogenase* (GAPDH; P04797), while *Malate dehydrogenase, cytoplasmic* (O88989), *L-lactate dehydrogenase A chain* (P04642) and GAPDH (P04797) were

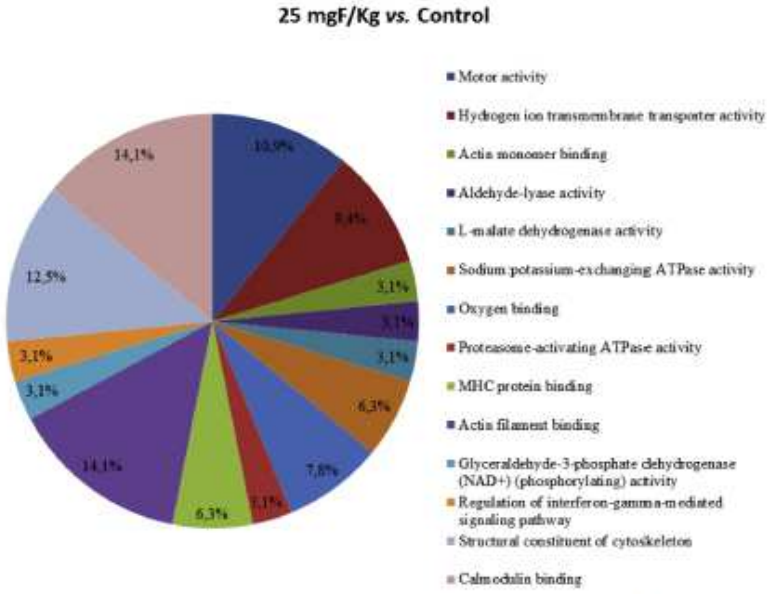

Fig. 2. Functional distribution of proteins identified with differential expression in the jejunum of rats exposed acute dose of 25 mgF/Kg wb *vs.* Control Group (0 mgF/L). Categories of proteins based on GO annotation Biological Process. Terms significant (Kappa = 0.04) and distribution according to percentage of number of genes. Proteins access number was provided by the UNIPROT. The gene ontology was evaluated according to ClueGo® pluggins of CYTOSCAPE® software 3.4.0 (Bindea et al., 2009, 2013).

also in the ileum upon exposure to F. These findings indicate a great impair in energy metabolism (especially of carbohydrates) in the jejunum and ileum of rats upon acute exposure to F, being the jejunum more affected than the ileum. These findings are somehow expected, since the enzymes involved in energy metabolism are highly affected by F, at least under chronic exposure to this ion (Araujo et al., 2019; Dionizio et al., 2018; Pereira et al., 2018). In addition, *ATP synthase subunit beta, mitochondrial (P10719)* and *ATP synthase subunit alpha, mitochondrial* (P15999), key enzymes in respiratory chain, were down regulated in the jejunum after acute F exposure, which corroborates the impair in the energy metabolism. It has been reported that expression of *ATP synthase subunit beta, mitochondrial* is reduced and correlated with ATP content in the livers of type 1 and type 2 diabetic mice, while hepatic overexpression of *ATP synthase subunit beta, mitochondrial* increases cellular ATP content and suppresses gluconeogenesis, leading to hyperglycemia amelioration (Wang et al., 2014).

Polyubiquitin C (Q63429) is a highly conserved polypeptide that is covalently bound to other cellular proteins to signal processes such as protein degradation, protein/protein interaction and protein intracellular trafficking (Ciechanover and Schwartz, 1998). In the present study, some of the above-mentioned proteins that interacted with GLUT4 also interacted with *Polyubiquitin C*. Another protein that interacted with *Polyubiquitin C* is Peroxiredoxin-1 (Q63716) that was absent in the jejunum upon acute exposure to F. Peroxiredoxin-1 plays an important role in cell protection against oxidative stress by detoxifying peroxides and acting as sensor of hydrogen peroxide-mediated signaling events (UniProt, 2019). In balance in the oxidant/antioxidant defense is a common effect of F (Araujo et al., 2019; Barbier et al., 2010; Iano et al., 2014).

MAPK3 (P21708) or extracellular-signal regulated kinases (ERK1) are a family of proteins that act as intermediaries in the signal transduction cascades triggered by extracellular signals at membrane receptors, through reversible protein phosphorylation, constituting one of the main mechanisms of cellular communication. They seem to be universal components of signal transduction mechanisms since multiple forms have been identified in a variety of organisms (Dinsmore and Soriano, 2018; Hymowitz and Malek, 2018). One of the proteins interacting with MAPK3 is *Transgelin-2*. Increase in this protein is associated with the development of cancer, while its suppression leads to inhibition of cell proliferation, invasion and metastasis (Yakabe et al., 2016). Recently, transgelin was shown to be increased in colorectal cancer (Zhou et al., 2018) and was suggested as a potential biomarker for cancer as well as a potential new target for cancer treatment (Meng et al., 2017). In our studies, *Transgelin-2* was increased in the jejunum after acute exposure to F, but was absent in the ileum after acute exposure to F. The reason for this differential pattern of expression is not apparent at the moment but could possibly be related to the different characteristics in intestine segments, which should be evaluated in further studies. Interestingly, another protein involved in the control of cell proliferation (*Stress-70 protein, mitochondrial*; P48721) was identified exclusively in the jejunum after acute F exposure. In the jejunum, *Stress-70 protein, mitochondrial* also interacted with *Heterogeneous nuclear ribonucleoprotein K* that was also an interacting player in the ileum. This protein is one of the major pre-mRNA-binding proteins, playing an important role in p53/TP53 response to DNA damage, acting at the level of both transcription activation and repression, being necessary for the induction of apoptosis. In the jejunum, another identified protein that interacted with *Heterogeneous nuclear ribonucleoprotein K* was *DEAD (Asp-Glu-Ala-Asp) box polypeptide 5* (DDX5; Q6AYI1), an RNA-binding protein overexpressed in various malignant tumors (Janknecht, 2010), since it causes growth (Saporita et al., 2011) and metastasis (Yang et al., 2006), through activation of several oncogenic pathways (Yang et al., 2006). In the present study, however, DDX5 was absent in the jejunum upon acute exposure to F. It has been reported that depletion of DDX5 causes apoptosis by inhibition of mammalian target of rapamycin complex 1 (mTORC1) (Taniguchi et al., 2016). Fluoride-induced apoptosis has been widely reported in the literature (Barbier et al., 2010; Ribeiro et al., 2017). In the ileum, *Elongation*

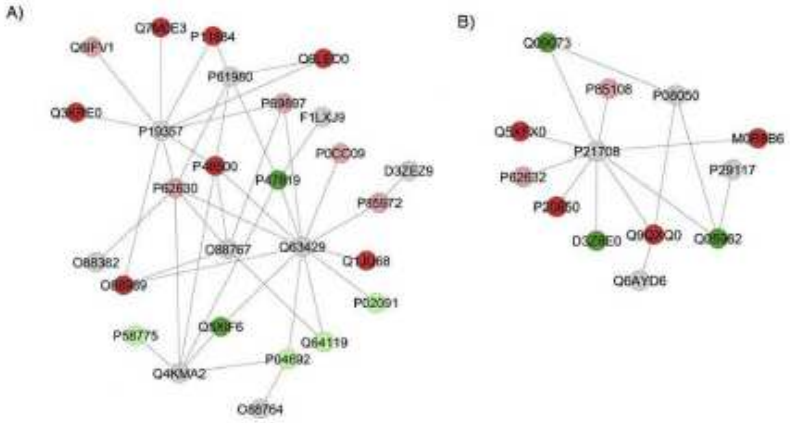

Fig. 3. Subnetworks created by ClusterMarker® to establish the interaction between proteins identified with differential expression in the 25 mgF/Kg wb group in relation to the control group in ileum. The color of the nodes indicates the differential expression of the respective named protein with its access code. The dark red and dark green nodes indicate proteins unique to the control and 25 mgF/Kg wb groups, respectively. The nodes in gray indicate the interaction proteins that are offered by CYTOSCAPE®, which were not identified in the present study and the light red and light green nodes indicate downregulation and upregulation, respectively. In A the access numbers in the gray nodes correspond to: *Solute carrier family 2, facilitated glucose transporter member 4* (P19357), *Heterogeneous nuclear ribonucleoprotein K* (P61960), *Membrane-associated guanylate kinase, WW and PDZ domain-containing protein 2* (O88382), *UV excision repair protein RAD23 homolog B* (Q4KMA2), *Protein deglycase DJ-1* (O88767), *Death-associated protein kinase 3* (O88764), *Polyubiquitin-C* (Q63429), *Protein Hprt* (F1LXJ9) and *Protein Svil* (D3ZEZ9). The access numbers of the unique proteins of the control (dark red nodes) correspond to the: *Destrin* (Q7M0E3), *Aldehyde dehydrogenase, mitochondrial* (P11884), *Histone H3.1* (Q6LED0), *ATPase family AAA domain-containing protein 3* (Q3KRE0), *Triosephosphate isomerase* (P48500), *Malate dehydrogenase, cytoplasmic* (O88989) and *Eukaryotic translation initiation factor 3 subunit A* (Q1JU68). The accession numbers of the unique 25 mgF/Kg wb (dark green nodes) proteins correspond to the: *Glial fibrillary acidic protein* (P47819) and *Tubulin alpha-4A chain* (Q5XIF6). The access numbers of the down regulated proteins (light red nodes) correspond to the: *Keratin, type I cytoskeletal 14* (Q6IFV1), *Tubulin beta-5 chain* (P68897), *Histone H2A type 2-A* (P0CC09), *Vinculin* (P85972) and *Elongation factor 1-alpha 1* (P62630). The access numbers of the downregulated proteins (light green nodes) correspond to the: *Hemoglobin subunit beta-1* (P02091), *Myosin light polypeptide 6* (Q64119), *Tropomyosin alpha-1 chain* (P04692) and *Tropomyosin beta chain* (P58775). In B the access numbers in the gray nodes correspond to: *Peptidyl-prolyl cis-trans isomerase F, mitochondrial* (P29117), *PDZ and LIM domain protein 2* (Q6AYD6), *Mitogen-activated protein kinase 3* (P21708) and *Gap junction alpha-1 protein* (P08050). The access numbers of the unique proteins of the control (dark red nodes) correspond to the: *Transgelin-2* (Q5XFX0), *Protein phosphatase 1A* (P20650), *Alpha-actinin-4* (Q9QXQ0) and *Protein Tubb1* (M0R8B6). The accession numbers of the unique 25 mgF/Kg wb (dark green nodes) proteins correspond to the: *ADP/ATP translocase 2* (Q09073), *ADP/ATP translocase 1* (Q05962) and *Ribosomal protein S6 kinase* (D3ZBE0). The access numbers of the downregulated proteins (light red nodes) correspond to the: *Tubulin beta-2A chain* (P85108) and *Elongation factor 1-alpha 2* (P62632). (For interpretation of the references to color in this figure legend, the reader is referred to the web version of this article.)

factor 1-alpha 1 (EF-1 αP62630) that interacted with *Heterogeneous nuclear ribonucleoprotein K* was reduced upon acute exposure to F, which is also related to induction of apoptosis, since elevated levels of EF-1 α are observed during neoplastic transformation and in tumors (Grant et al., 1992). In-line with this, *Aldehyde dehydrogenase, mitochondrial* (ALDH2; P11884) was absent upon acute exposure to F. Pharmacological inhibition of ALDH2 *per se* induces mitochondrial dysfunction and cell death (Mali et al., 2016). These findings are important because some reports incorrectly associate F exposure with the incidence of osteosarcoma (Bassin et al., 2006; Rameshet al., 2001) and bladder cancer (Grandjean et al., 1992). Our findings, however, give additional support to the safety of use of F on this aspect, since even when administered in a high dose as in the present study, F causes alterations in several proteins that lead to apoptosis instead of cell proliferation.

Most of the proteins that interacted with MAPK3 both in the jejunum and ileum are associated with cytoskeleton and some of them are actin-binding proteins (ABPs). Actin is one of the most abundant proteins in eukaryotic cells, participating in different cellular processes such as cell differentiation, proliferation, apoptosis, migration and signaling (Kristo et al., 2016). ABPs are highly abundant and directly participate in the modulation of cell processes through the regulation of actin cytoskeleton (Artman et al., 2014). Interestingly, *Transgelin-2* (Q5XFX0), an ABP, was absent in the ileum, but identified exclusively in the jejunum after acute exposure to F. This protein regulates the actin cytoskeleton through actin binding and sometimes participates in cytoskeleton remodeling (Dvorakova et al., 2014). In line with this, it is important to highlight that the categories with the highest percentage of associated genes, as revealed by functional classification, were acting filament binding (14.1%) and calmodulin binding (14.1%) for the jejunum (Fig. 2) and organization of intermediary filaments (21%) for the ileum (Fig. 4). Alterations in proteins involved in the cytoskeleton might explain some of the morphological findings of the present study. Both in the jejunum and ileum, the thickness of the tunica muscularis was significantly decreased in the group that received the acute dose of F, when compared with control This alteration is considered as one of the possible explanations for the impairment of the intestinal motility upon exposure to F (Viteri and Schneider, 1974). For the inhibitory control of the motility, the main neurotransmitters involved are NO and VIP (Benarroch, 2007). In this sense, in our study NO was decreased in both segments, while VIP was increased in the jejunum and decreased in the ileum. These findings agree with those found by our group in the duodenum (Melo et al., 2017) and jejunum (Dionizio et al., 2018) of rats chronically treated with water containing 10 and 50 mgF/L.

Contrarily to which was seen in the chronic treatment of jejunum (Dionizio et al., 2018) and ileum (unpublished data), upon the acute exposure to F the organism might not have had time to adapt to its toxic effect, which means that the loss of energy may have not been repaired. According to the literature, some of the initial symptoms of acute toxicity are generalized weakness, drop in blood pressure and disorientation (Buzalaf and Whitford, 2011; Whitford, 2011), which might be caused by decreased energy levels in the body.

In summary, our results, when analyzed in conjunction, suggest that the gastrointestinal symptoms found in cases of acute F exposure might be related to the morphological alterations in the gut (decrease in the thickness of the tunica muscularis) that, at the molecular level, can be explained by alterations in the gut vipergic innervation and in proteins

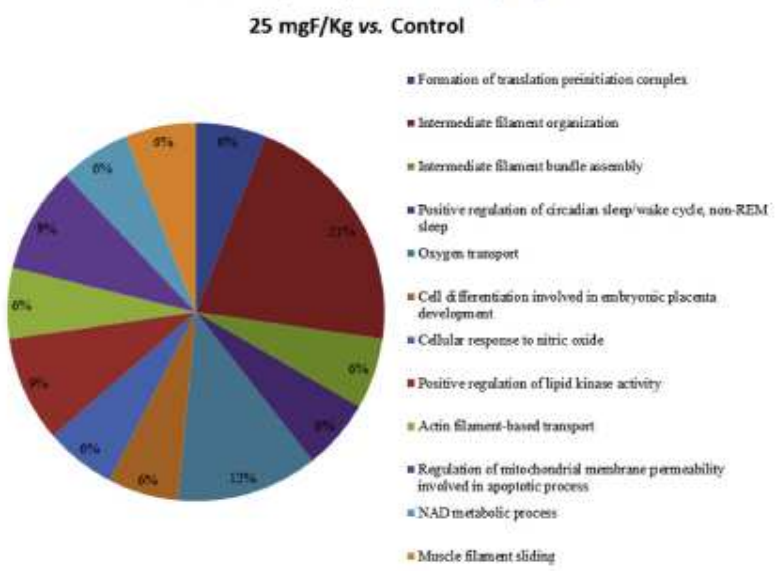

Fig. 4. Functional distribution of proteins identified with differential expression in the ileum of rats exposed acute dose of 25 mgF/Kg wh vs. Control Group (0 mgF/L). Categories of proteins based on GO annotation Biological Process. Terms significant (Kappa = 0.04) and distribution according to percentage of number of genes. Proteins access number was provided by the UNIPROT. The gene ontology was evaluated according to ClueGo® plugin's of CYTOSCAPE® software 3.4.0 (Bindea et al., 2009, 2013).

that regulate the cytoskeleton. These findings help to explain the gastrointestinal signs and symptoms reported in cases of acute F toxicity.

Supplementary data to this article can be found online at https://doi.org/10.1016/j.scitotenv.2020.140419.

CRediT authorship contribution statement

Aline Dionizio: Writing - review & editing, Writing - original draft, Formal analysis, Validation, Investigation, Data curation, Funding acquisition, Methodology. **Carina Guimarães Souza Melo:** Writing - original draft, Formal analysis, Investigation, Methodology, Funding acquisition. **Isabela Tomazini Sabino-Arias:** Data curation, Formal analysis. **Tamara Teodoro Araujo:** Data curation, Formal analysis. **Talita Mendes Silva Ventura:** Data curation, Formal analysis. **Aline Lima Leite:** Data curation, Formal analysis. **Sara Raquel Garcia Souza:** Data curation, Formal analysis. **Erika Xavier Santos:** Data curation, Formal analysis. **Alessandro Domingues Heubel:** Data curation, Formal analysis. **Juliana Gadelha Souza:** Data curation, Formal analysis. **Juliana Vanessa Colombo Martins Perles:** Data curation, Formal analysis, Investigation, Methodology. **Jacqueline Nelisis Zanoni:** Data curation, Formal analysis, Investigation, Methodology. **Marília Afonso Rabelo Buzalaf:** Writing - review & editing, Formal analysis, Writing - original draft, Methodology, Funding acquisition Project administration, Supervision.

Declaration of competing interest

The authors declare that they have no known competing financial interests or personal relationships that could have appeared to influence the work reported in this paper.

Acknowledgements

This study was supported by FAPESP (2011/10233-7, 2012/16840-5 and 2016/09100-6).

References

Araujo, T.T., Barbosa Silva Pereira, H.A., Dionizio, A., Sanchez, C.D.C., de Souza Carvalho, T., da Silva Fernandes, M., et al., 2019. Changes in energy metabolism induced by fluoride: insights from inside the mitochondria. Chemosphere 236, 124357.

Artman, L., Dormoy-Raclet, V., von Roretz, C., Gallouzi, I.E., 2014. Planning your every move: the role of beta-actin and its post-transcriptional regulation in cell motility. Semin. Cell Dev. Biol. 34, 33–43.

Barbier, O., Arreola-Mendoza, L., Del Razo, L.M., 2010. Molecular mechanisms of fluoride toxicity. Chem. Biol. Interact. 188, 319–333.

Bassin, E.B., Wypij, D., Davis, R.B., Mittleman, M.A., 2006. Age-specific fluoride exposure in drinking water and osteosarcoma (United States). Cancer Causes Control. 17, 421–428.

Bauer-Mehren, A., 2013. Integration of genomic information with biological networks using Cytoscape. Methods Mol. Biol. 1021, 37–61.

Benarroch, E.E., 2007. Enteric nervous system - functional organization and neurologic implications. Neurology 69, 1953–1957.

Bindea, G., Bernhard, M., Hubert, H., Pornpimol, C., Marie, T., Amos, K., Wolf-Herman, F., Franck, P., Zlatko, T., Bindea, G., Galon, J., 2009. ClueGO: a Cytoscape plug-in to decipher functionally grouped gene ontology and pathway annotation networks. Bioinformatics 25 (8), 1091–1093. https://doi.org/10.1093/bioinformatics/btp101.

Bindea, G., Galon, J., Mlecnik, B., 2013. CluePedia Cytoscape plugin: pathway insights using integrated experimental and in silico data. Bioinformatics 29 (5), 661–663. https://doi.org/10.1093/bioinformatics/btt019.

Bradford, M.M., 1976. A rapid and sensitive method for the quantitation of microgram quantities of protein utilizing the principle of protein-dye binding. Anal. Biochem. 72, 248–254.

Buzalaf, M.A., Whitford, G.M., 2011. Fluoride metabolism. Monogr. Oral Sci. 22, 20–36.

Buzalaf, M.A., Moraes, C.M., Olympio, K.P., Pessan, J.P., Grizzo, L.T., Silva, T.L., et al., 2013. Seven years of external control of fluoride levels in the public water supply in Bauru, Sao Paulo, Brazil. J. Appl. Oral Sci. 21, 92–98.

Ciechanover, A., Schwartz, A.L., 1998. The ubiquitin-proteasome pathway: the complexity and myriad functions of proteins death. Proc. Natl. Acad. Sci. U. S. A. 95, 2727–2730.

Dinsmore, C.J., Soriano, P., 2018. MAPK and PI3K signaling: at the crossroads of neural crest development. Dev. Biol. (Suppl. 1), 579–597.

Dionizio, A., Pereira, H., Araujo, T.T., Sabino-Arias, I.T., Fernandes, M.S., Oliveira, K.A., et al., 2019. Effect of duration of exposure to fluoride and type of diet on lipid parameters and de novo lipogenesis. Biol. Trace Elem. Res. 190, 157–171.

Dionizio, A.S., Melo, C.G.S., Sabino-Arias, I.T., Ventura, T.M.S., Leite, A.L., Souza, S.R.G., et al., 2018. Chronic treatment with fluoride affects the jejunum: insights from proteomics and enteric innervation analysis. Sci. Rep. 8, 3180.

Dunipace, A.J., Brizendine, E.J., Zhang, W., Wilson, M.E., Miller, L.L., Katz, B.P., et al., 1995. Effect of aging on animal response to chronic fluoride exposure. J. Dent. Res. 74, 358–368.

Dvorakova, M., Nenutil, R., Bouchal, P., 2014. Transgelins, cytoskeletal proteins implicated in different aspects of cancer development. Expert Rev Proteomics 11, 149–165.

Grandjean, P., Olsen, J.H., Jensen, O.M., Juel, K., 1992. Cancer incidence and mortality in workers exposed to fluoride. J. Natl. Cancer Inst. 84, 1903–1909.

Grant, A.G., Flomen, R.M., Tizard, M.L., Grant, D.A., 1992. Differential screening of a human pancreatic adenocarcinoma lambda gt11 expression library has identified increased transcription of elongation factor EF-1 alpha in tumour cells. Int. J. Cancer 50, 740–745.

He, L.F., Chen, J.G., 2006. DNA damage, apoptosis and cell cycle changes induced by fluoride in rat oral mucosal cells and hepatocytes. World J. Gastroenterol. 12, 1144–1148.

Hymowitz, S.G., Malek, S., 2018. Targeting the MAPK pathway in RAS mutant cancers. Cold Spring Harb Perspect Med 8, a031492.

Iano, F.G., Ferreira, M.C., Quaggio, C.B., Fernandes, M.S., Oliveira, R.C., Ximenes, V.F., et al., 2014. Effects of chronic fluoride intake on the antioxidant systems of the liver and kidney in rats. J. Fluor. Chem. 168, 212–217.

Jankowski, R., 2010. Multi-talented DEAD-box proteins and potential tumor promoters: p68 RNA helicase (DDX5) and its paralog, p72 RNA helicase (DDX17). Am. J. Transl. Res. 2, 223–234.

Jimenez-Cordova, M.I., Gonzalez-Horta, C., Ayllon-Vergara, J.C., Arreola-Mendoza, L., Aguilar-Madrid, G., Villareal-Vega, E.E., et al., 2019. Evaluation of vascular and kidney injury biomarkers in Mexican children exposed to inorganic fluoride. Environ. Res. 169, 220–228.

Kristo, I., Bajusz, I., Bajusz, C., Borkuti, P., Vilmos, P., 2016. Actin, actin-binding proteins, and actin-related proteins in the nucleus. Histochem. Cell Biol. 145, 373–388.

Lima Leite, A., Guilhume Vaz Madureira Lobo, J., Barbosa da Silva Pereira, H.A., Silva Fernandes, M., Martini, T., Zucki, F., et al., 2014. Proteomic analysis of gastrocnemius muscle in rats with streptozotocin-induced diabetes and chronically exposed to fluoride. PLoS One 9, e106646.

Lobo, J.G., Leite, A.L., Pereira, H.A., Fernandes, M.S., Peres-Buzalaf, C., Sumida, D.H., et al., 2015. Low-level fluoride exposure increases insulin sensitivity in experimental diabetes. J. Dent. Res. 94, 990–997.

Mali, V.R., Deshpande, M., Pan, G., Thandavarayan, R.A., Palaniyandi, S.S., 2016. Impaired ALDH2 activity decreases the mitochondrial respiration in H9C2 cardiomyocytes. Cell. Signal. 28, 1–6.

McDonagh, M.S., Whiting, P.F., Wilson, P.M., Sutton, A.J., Chestnutt, I., Cooper, J., et al., 2000. Systematic review of water fluoridation. BMJ 321, 855–859.

Melo, C.C.S., Perles, J., Zanoni, J.N., Souza, S.R.G., Santos, E.X., Leite, A.L., et al., 2017. Enteric innervation combined with proteomics for the evaluation of the effects of chronic fluoride exposure on the duodenum of rats. Sci. Rep. 7, 1070.

Meng, T., Liu, L., Hao, R., Chen, S., Dong, Y., 2017. Transgelin-2: a potential oncogenic factor. Tumour Biol. 39, 1010428317702650.

Millan, P.P., 2013. Visualization and analysis of biological networks. Methods Mol. Biol. 1021, 63–88.

Mitsui, C., Dote, T., Adachi, K., Dote, E., Fujimoto, K., Shimbo, Y., et al., 2007. Harmful effects and acute lethal toxicity of intravenous administration of low concentrations of hydrofluoric acid in rats. Toxicol. Ind. Health 23, 5–12.

Mitsui, C., Dote, T., Yamadori, E., Imanishi, M., Nakayama, S., Ohnishi, K., et al., 2010. Toxicokinetics and metabolism deteriorated by acute nephrotoxicity after a single intravenous injection of hydrofluoric acid in rats. J. Occup. Health 52, 395–399.

Mullenix, P.J., Denbesten, P.K., Schunior, A., Kernan, W.J., 1995. Neurotoxicity of sodium fluoride in rats. Neurotoxicol. Teratol. 17, 169–177.

Nopakun, J., Messer, H.H., Voller, V., 1989. Fluoride absorption from the gastrointestinal tract of rats. J. Nutr. 119, 1411–1417.

Orchard, S., 2012. Molecular interaction databases. Proteomics 12, 1656–1662.

Panneerselvam, L., Raghunath, A., Sundarraj, K., Perumal, E., 2019. Acute fluoride exposure alters myocardial redox and inflammatory markers in rats. Mol. Biol. Rep. 46, 6155–6164.

Pereira, H., Dionizio, A.S., Araujo, T.T., Fernandes, M.D.S., Iano, F.G., Buzalaf, M.A.R., 2018. Proposed mechanism for understanding the dose- and time-dependency of the effects of fluoride in the liver. Toxicol. Appl. Pharmacol. 358, 68–75.

Pereira, H.A., Leite Ade, L., Charone, S., Lobo, J.G., Cestari, T.M., Peres-Buzalaf, C., et al., 2013. Proteomic analysis of liver in rats chronically exposed to fluoride. PLoS One 8, e75343.

Pereira, H.A., Dionizio, A.S., Fernandes, M.S., Araujo, T.T., Cestari, T.M., Buzalaf, C.P., et al., 2016. Fluoride intensifies hypercaloric diet-induced ER oxidative stress and alters lipid metabolism. PLoS One 11, e0158121.

Ramesh, N., Vijayaraghavan, A.S., Desai, B.S., Natarajan, M., Murthy, P.B., Pillai, K.S., 2001. Low levels of p53 mutations in Indian patients with osteosarcoma and the correlation with fluoride levels in bone. J. Environ. Pathol. Toxicol. Oncol. 20 (2), 7–43.

Ribeiro, D.A., Cardoso, C.M., Yujra, V.Q., M, D.E.BV., Aguiar Jr., O., Pisani, L.P., et al., 2017. Fluoride induces apoptosis in mammalian cells: in vitro and in vivo studies. Anticancer Res. 37, 4767–4777.

Santoyo-Sanchez, M.P., del Carmen Silva-Lucero, M., Arreola-Mendoza, L., Barbier, O.C., 2013. Effects of acute sodium fluoride exposure on kidney function, water homeostasis, and renal handling of calcium and inorganic phosphate. Biol. Trace Elem. Res. 152, 367–372.

Saporita, A.J., Chang, H.C., Winkeler, C.L., Apicelli, A.J., Kladney, R.D., Wang, J., et al., 2011. RNA helicase DDX5 is a p53-independent target of ARF that participates in ribosome biogenesis. Cancer Res. 71, 6708–6717.

Shanthakumari, D., Srinivasalu, S., Subramanian, S., 2004. Effect of fluoride intoxication on lipidperoxidation and antioxidant status in experimental rats. Toxicology 204, 219–228.

Suarez, P., Quintana, M.C., Hernandez, L., 2008. Determination of bioavailable fluoride from sepiolite by "in vivo" digestibility assays. Food Chem. Toxicol. 46, 480–488.

Taniguchi, T., Iizumi, Y., Watanabe, M., Masuda, M., Morita, M., Aono, Y., et al., 2016. Resveratrol directly targets DDX5 resulting in suppression of the mTORC1 pathway in prostate cancer. Cell Death Dis. 7, e2211.

UniProt C, 2019. UniProt: a worldwide hub of protein knowledge. Nucleic Acids Res. 47, D506–D515.

Viteri, F.E., Schneider, R.E., 1974. Gastrointestinal Alterations in Protein-Calorie Malnutrition. Med. Clin. North Am. 58 (6), 1487–1505. https://doi.org/10.1016/s0025-7125(16)32085-5.

Wang, C., Chen, Z., Li, S., Zhang, Y., Jia, S., Li, J., et al., 2014. Hepatic overexpression of ATP synthase beta subunit activates PI3K/Akt pathway to ameliorate hyperglycemia of diabetic mice. Diabetes 63, 947–959.

Whitford, G.M., 1992. Acute and chronic fluoride toxicity. J. Dent. Res. 71, 1249–1254.

Whitford, G.M., 1996. The metabolism and toxicity of fluoride. Monogr. Oral Sci. 16 (Rev 2), 1–153.

Whitford, G.M., 2011. Acute toxicity of ingested fluoride. Monogr. Oral Sci. 22, 66–80.

Whitford, G.M., Pashley, D.H., 1984. Fluoride absorption: the influence of gastric acidity. Calcif. Tissue Int. 36, 302–307.

Wong, M.C., Clarkson, J., Glenny, A.M., Lo, E.C., Marinho, V.C., Tsang, B.W., et al., 2011. Cochrane reviews on the benefits/risks of fluoride toothpastes. J. Dent. Res. 90, 573–579.

Yakabe, K., Murakami, A., Kajimura, T., Nishimoto, Y., Sueoka, K., Sato, S., et al., 2016. Functional significance of transgelin-2 in uterine cervical squamous cell carcinoma. J. Obstet. Gynaecol. Res. 42, 566–572.

Yan, X., Yan, X., Morrison, A., Han, T., Chen, Q., Li, J., et al., 2011. Fluoride induces apoptosis and alters collagen I expression in rat osteoblasts. Toxicol. Lett. 200, 133–138.

Yang, L., Lin, C., Liu, Z.R., 2006. P68 RNA helicase mediates PDGF-induced epithelial mesenchymal transition by displacing Axin from beta-catenin. Cell 127, 139–155.

Zhou, H., Zhang, Y., Wu, L., Xie, W., Li, L., Yuan, Y., et al., 2018. Elevated transgelin/TNS1 expression is a potential biomarker in human colorectal cancer. Oncotarget 9, 1107–1113.